

# PARAMETRIC MODELLING OF SPARSE RANDOM TREES USING 3D COPULAS

DAVID NEUHÄUSER\*, CHRISTIAN HIRSCH\*, CATHERINE GLOAGUEN\*\*, AND VOLKER SCHMIDT\*

ABSTRACT. We provide a parametric modelling approach suitable for various kinds of hierarchical networks based on random geometric graphs. In these networks, we have two kinds of components, so-called high-level components (HLC) and low-level components (LLC). Each HLC is associated with a serving zone and all LLC within this area are connected to the corresponding HLC. So-called sparse LLC networks, where only few LLC occur in the typical serving zone, are a non-negligible subdomain when investigating hierarchical networks. Therefore, we supply distributional results for structural characteristics where two LLC are independently and uniformly distributed along the segment system of the typical serving zone. In particular, we are interested in the joint distribution of three quantities, namely the length of the joint part of the shortest paths from the LLC to the HLC as well as the lengths of the corresponding disjoint remaining parts. In order to provide a parametric, three-dimensional distribution function for these random variables, we utilise a pseudo-maximum likelihood approach. More precisely, we fit parametric approximation formulas to the marginal density functions as well as parametric copula functions which match with the observed correlation structure. We also provide an asymptotic result for the joint distribution of the connection lengths as the size of the typical cell increases unboundedly. This general modelling approach is explicitly explained for the case that the random geometric graph is formed by the edges of random tessellations.

## 1. INTRODUCTION

All kinds of network systems, e.g. transport and traffic networks, telecommunication networks, electricity networks and even networks in materials science, depend on the nodes and connection paths between these nodes [3, 19]. From the mathematical point of view, these networks can be represented by several kinds of geometric graphs, provided that the networks fulfill certain conditions. For various – partly very different – reasons, people are interested in point-to-point distances in such graphs which are measured along the connecting edge system between the nodes of the network. In the present paper, we focus on a special kind of hierarchical networks whose components are located on the edge system of a random geometric graph and present a parametric modelling approach for multivariate point-to-point distances. In particular, our networks can be decomposed into two levels of hierarchy, i.e., path connections within those networks are always investigated between high-level components (HLC) and low-level components (LLC). For instance, in the context of telecommunication networks, HLC correspond to wire-centre-stations whereas LLC represent service-area-interfaces or subscribers. For an exhaustive investigation of large and complex fixed access telecommunication networks in urban and also rural regions, it is not sufficient to consider just *dense LLC networks*, i.e., networks with numerous low-level components within a serving zone as we did for instance in [21]. It is also necessary to take networks into account where only few LLC are located within a supply area of a corresponding HLC. Such networks are called *sparse LLC networks*. Recall that tracing the shortest paths from each LLC in one serving zone to the corresponding HLC will yield a natural tree structure, see [20, 21]. For the simplest cases of sparse LLC networks, e.g., for two LLC within an HLC's serving zone, it is – in contrast to the dense LLC network

---

2000 *Mathematics Subject Classification.* 60D05, 62E17, 65C05, 65C50.

*Key words and phrases.* Sparse LLC networks, joint distribution, parametric copula, pseudo-maximum-likelihood, typical serving zone, network planning, limit theorem.

\*Institute of Stochastics, Ulm University, 89069 Ulm, Germany; E-mail: david.neuhaeuser@uni-ulm.de.

\*\*Orange Labs, 92794 Issy-Moulineaux Cedex 9, France.

– relatively easy to provide a complete description of the corresponding shortest-path tree. Complete description means explicitly considering *each* occurring path from an LLC to the HLC, something which is in the dense LLC network not possible because of the large number of LLC nodes. The main goal of the present paper is to fully describe the shortest-path tree  $G$  for a sparse LLC network consisting of two LLC. In particular, this goal can be achieved by investigating the three random variables  $M_{1\wedge 2}$ , denoting the length of the joint part of the shortest paths from the LLC to the HLC, as well as  $M_1$  and  $M_2$ , representing the lengths of the corresponding disjoint remaining parts. Furthermore, we show that for an unboundedly increasing size of the serving zone, the asymptotic distribution of the shortest-path tree admits a simple geometric description. Regarding asymptotic properties of shortest-path trees of dense LLC networks, we refer to [11, 21].

The paper is organised as follows. Section 2 provides basic notation and mathematical tools of stochastic geometry used in the present paper. In particular, the flexible and established *stochastic subscriber line model* is briefly recalled. Besides, a suitable modelling approach for a parametric three-dimensional joint distribution function of  $M = (M_1, M_2, M_{1\wedge 2})$  is given. Then, in Section 3, we show the results of our modelling approach. Approximative formulas for the univariate marginal densities of  $M$  as well as copula functions are presented. Furthermore, besides visual comparison to empirical data, we provide multivariate test results on equality of distribution in order to validate our modelled data. In Section 4, we investigate the limiting distributional behaviour of  $G$  as the linear intensity of the HLC tends to 0. Finally, Section 5 concludes the paper and gives an outlook to possible future research.

## 2. MATHEMATICAL FRAMEWORK AND MODELLING APPROACH

**2.1. The stochastic subscriber line model.** During the last years, the *stochastic subscriber line model* (SSLM) has turned out to be a suitable and reliable tool for modelling fixed access networks. For the convenience of the reader, the most important characteristics are listed and briefly discussed in the following. For details on this already thoroughly investigated stochastic model, the reader is referred to [20, 21] and also [26]. Stochastic geometry with a variety of useful characteristics and features can also be utilised to provide related models which frequently play an important role in the analysis of mobile telecommunication networks [2] and also the assessment of traffic incident risks [22].

**2.1.1. Underlying road system.** The underlying road system, along which the cables of the telecommunication network are installed, is represented by a stationary random tessellation  $T$  defined on some probability space  $(\Omega, \mathcal{F}, \mathbb{P})$ . In the present paper, we assume  $T$  to be either a Poisson-Voronoi tessellation (PVT), a Poisson-Delaunay tessellation (PDT) or a Poisson line tessellation (PLT). These types of tessellations turned out to represent the underlying road system sufficiently well [21]. The edge system of  $T$  is denoted by  $T^{(1)}$ , its length intensity is given by  $\gamma = \mathbb{E} \nu_1(T^{(1)} \cap [0, 1]^2)$ , where  $\nu_1$  denotes the one-dimensional Hausdorff measure. For the analysis of connection lengths in telecommunication networks, it is useful to investigate the network distribution from the perspective of a randomly chosen access point on the road system. This can be made precise by defining the Palm version  $T^*$  of  $T$ . Its distribution is given by the representation formula

$$\mathbb{E}h(T^*) = \frac{1}{\gamma} \mathbb{E} \int_{T^{(1)} \cap [0, 1]^2} h(T - x) \nu_1(dx),$$

where  $h : \mathbb{T} \rightarrow [0, \infty)$  is any measurable function and  $\mathbb{T}$  denotes the family of tessellations in  $\mathbb{R}^2$ . Detailed information about these random geometric graphs can be found in [6, 24].

**2.1.2. High-level components.** Considering the Palm version  $T^*$  corresponds to assuming that an HLC is located at the origin. The remaining HLC are modelled by a Cox point process  $X_H$  whose atoms are located along  $T^{*,(1)}$ , the edge set of  $T^*$ . The random intensity measure of this Cox point process is proportional to  $\nu_1$  on  $T^{*,(1)}$ , i.e.,  $\mathbb{E}X_H(B) = \lambda_\ell \mathbb{E} \nu_1(T^{*,(1)} \cap B)$  for some linear intensity  $\lambda_\ell$  and some Borel set  $B \subset \mathbb{R}^2$ . In other words, given  $T^{*,(1)}$  the point process

$X_H$  is a homogeneous Poisson point process on  $T^{*(1)}$ . Detailed, additional information about various types of point processes can be found in [7] and [13].

2.1.3. *Typical serving zone.* The typical serving zone  $\Xi_H^*$  and the typical segment system  $S_H^*$  are loosely speaking representatives for all serving zones (the supply areas of the HLC) and their corresponding segment systems of a city. Formally,  $\Xi_H^*$  is the zero-cell of the Voronoi tessellation induced by  $X_H \cup \{o\}$ , where  $o = (0, 0)$  denotes the origin. Besides,  $S_H^* = \Xi_H^* \cap T^{*(1)}$ . Additional information about Palm theory and typical marks can be found in [6, 7]. In the following, the segments of  $S_H^*$  are denoted by  $R_1, \dots, R_N$ . Note that the number  $N$  of segments may be different from one realisation of  $S_H^*$  to another one. Thus,  $N$  is a random variable, as well.

2.1.4. *Low-level components.* Modelling LLC in sparse networks is a little different to the method used in the SSLM so far. We put a *fixed* small number of LLC – in the present paper two – independently and uniformly distributed along  $S_H^*$ , i.e., for the locations  $L_i, i \in \{1, 2\}$ , it holds

$$L_i \sim \frac{\nu_1(\cdot \cap S_H^*)}{\nu_1(S_H^*)}.$$

In order to simulate these  $L_i$ , we proceed in the following way.

- (i) Simulate  $\Lambda_i \sim U[0, \sum_{j=1}^N \nu_1(R_j)]$ .
- (ii) Set  $\tilde{\Lambda}_i = \Lambda_i - \sum_{j=1}^{D_i} \nu_1(R_j)$  where  $D_i = \max\{k : 0 \leq k \leq N - 1, \sum_{j=1}^k \nu_1(R_j) < \Lambda_i\}$ .
- (iii) Take the two end points  $P_{B,i} = (x_{B,i}, y_{B,i})$  and  $P_{E,i} = (x_{E,i}, y_{E,i})$  of the  $(D_i + 1)$ -th segment of  $S_H^*$ .
- (iv) Put  $L_i = (x_{B,i}, y_{B,i}) + \tilde{\Lambda}_i \cdot (x_{E,i} - x_{B,i}, y_{E,i} - y_{B,i})$ .

2.1.5. *Shortest-path tree.* The shortest-path tree in a dense LLC network is roughly speaking a rearrangement of the typical segment system  $S_H^*$  [21]. In such a network, following the paths from all points in  $S_H^*$  to the origin  $o$  in the typical serving zone  $\Xi_H^*$  induces a natural tree structure. Note that shortest paths can leave  $\Xi_H^*$ . Similarly, in a sparse LLC network with a fixed number of LLC in  $\Xi_H^*$ , the shortest-path tree  $G$  is given by following the paths from the LLC to the origin. If shortest paths do not leave  $\Xi_H^*$ , then  $G$  is a strict subset of  $S_H^*$ , see Figure 2.1. We stress that also in the sparse scenario, shortest paths can leave  $\Xi_H^*$  and therefore, in Monte Carlo simulations it is not enough to only generate  $S_H^*$  but the tessellation needs to be constructed also in some suitable environment.

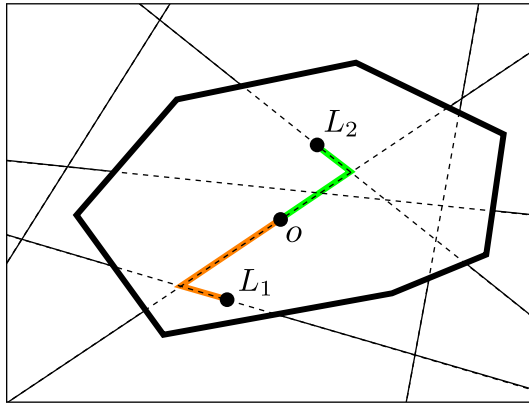


FIGURE 2.1. Shortest-path tree  $G$  in a sparse LLC network with two LLC as union of the orange and green branches fulfilling  $G \subsetneq S_H^*$  (dashed)

Knowing the three quantities length of the joint part of the shortest paths from the LLC to the origin as well as the lengths of the corresponding disjoint remaining parts gives us the whole shortest-path tree in the sparse scenario.

**2.2. Modelling approach for a direct simulation of the shortest-path tree.** In the following, we provide an approach to directly simulate the shortest-path tree  $G$  in a sparse LLC network by means of parametric copulas. This enables us to avoid time-consuming Monte Carlo simulations with subsequently extracting needed information out of  $S_H^*$ .

*2.2.1. A random vector representing the shortest-path tree.* As already mentioned in Section 2.1, in the present paper, we restrict the sparse LLC network to scenarios with only two occurring LLC. Nevertheless, this configuration already leads to quite substantial results. In the following, we write  $p(o, L_i)$  for the shortest path from the origin  $o$  to the LLC  $L_i, i \in \{1, 2\}$ , in the graph-theoretic sense, i.e., the shortest point-to-point connection measured along  $T^{*,(1)}$ . Then, we define the random variables  $M_1, M_2$  and  $M_{1\wedge 2}$ , depending on the locations of both LLC, as follows. We put

$$\begin{aligned} M_1 &= \nu_1(p(o, L_1) \setminus (p(o, L_1) \cap p(o, L_2))), \\ M_2 &= \nu_1(p(o, L_2) \setminus (p(o, L_1) \cap p(o, L_2))) \end{aligned}$$

and

$$M_{1\wedge 2} = \nu_1(p(o, L_1) \cap p(o, L_2)).$$

Besides, we define the trivariate random vector  $M = (M_1, M_2, M_{1\wedge 2})$ . The main goal of the present paper is to find a parametric three-dimensional joint distribution of  $M$  in order to have the ability of directly sampling the shortest-path tree  $G$  in a sparse LLC network, without having to simulate the typical serving zone and its corresponding segment system. Note that for sparse LLC networks with three or more LLC, it is difficult to recover the tree structure from the edge lengths of the tree. However, if only two LLC are located on the typical segment system, then also the structure of the tree is uniquely determined by  $M_1, M_2$  and  $M_{1\wedge 2}$ . Three possible scenarios are explained in Section 3.

*2.2.2. Preprocessing extracted data and subsequent pseudo-maximum-likelihood approach.* Due to some peculiarities in the structure of the realisations of  $M$  which are obtained by extraction out of  $S_H^*$ , we have to prepare the empirical data properly. First, since  $\mathbb{P}(M_{1\wedge 2} = 0) > 0$ , it is reasonable to distinguish between the two cases  $M_{1\wedge 2} = 0$  and  $M_{1\wedge 2} \neq 0$ . If  $M_{1\wedge 2} = 0$ , it is sufficient to consider the bivariate distribution function of  $(M_1, M_2)$  and adding a zero in the third component of  $M$ . Second, if  $M_{1\wedge 2} \neq 0$ , we have to distinguish between  $p(o, L_i) \subset p(o, L_j)$  and  $p(o, L_i) \not\subset p(o, L_j)$  where  $i, j \in \{1, 2\}$  and  $i \neq j$ . In particular, we denote by  $S$  the event  $(p(o, L_1) \subset p(o, L_2)) \cup (p(o, L_2) \subset p(o, L_1))$  and by  $S^c$  its complementary event,  $(p(o, L_1) \not\subset p(o, L_2)) \cap (p(o, L_2) \not\subset p(o, L_1))$ . If  $S$  occurs, again a two-dimensional distribution function is sufficient, whereas if its complement  $S^c$  occurs, it is mandatory to consider a three-dimensional copula, see Sections 3.2 and 3.3. Using the law of total probability, we can rewrite the distribution function  $F_M$  of  $M$  as follows.

$$\begin{aligned} F_M(x) &= \mathbb{P}(M_1 \leq x_1, M_2 \leq x_2, M_{1\wedge 2} \leq x_3) \\ &= \rho_1 \cdot \mathbb{P}(M_1 \leq x_1, M_2 \leq x_2, M_{1\wedge 2} \leq x_3 \mid M_{1\wedge 2} = 0) \\ &\quad + \rho_2 \cdot \mathbb{P}(M_1 \leq x_1, M_2 \leq x_2, M_{1\wedge 2} \leq x_3 \mid (M_{1\wedge 2} \neq 0) \cap S) \\ &\quad + \rho_3 \cdot \mathbb{P}(M_1 \leq x_1, M_2 \leq x_2, M_{1\wedge 2} \leq x_3 \mid (M_{1\wedge 2} \neq 0) \cap S^c), \end{aligned}$$

where  $x = (x_1, x_2, x_3) \in [0, \infty)^3$ ,  $\rho_1 = \mathbb{P}(M_{1\wedge 2} = 0)$ ,  $\rho_2 = \mathbb{P}((M_{1\wedge 2} \neq 0) \cap S)$ ,  $\rho_3 = \mathbb{P}((M_{1\wedge 2} \neq 0) \cap S^c)$  and  $\sum_{k=1}^3 \rho_k = 1$ . This partitioning of the distribution function  $F_M$  into a mixture of the conditional distributions

$$\begin{aligned} \varphi_1(x) &= \mathbb{P}(M_1 \leq x_1, M_2 \leq x_2, M_{1\wedge 2} \leq x_3 \mid M_{1\wedge 2} = 0), \\ \varphi_2(x) &= \mathbb{P}(M_1 \leq x_1, M_2 \leq x_2, M_{1\wedge 2} \leq x_3 \mid (M_{1\wedge 2} \neq 0) \cap S) \end{aligned}$$

and

$$\varphi_3(x) = \mathbb{P}(M_1 \leq x_1, M_2 \leq x_2, M_{1\wedge 2} \leq x_3 \mid (M_{1\wedge 2} \neq 0) \cap S^c)$$

has a great advantage which reads as follows. The mixing probabilities  $\rho_k, k \in \{1, 2, 3\}$ , can be easily estimated by

$$\hat{\rho}_k = \frac{\# \text{ simulations of scenario } k}{n},$$

and we can now proceed analogously to the 2D copula approach in [21] when fitting each of the three distribution functions  $\varphi_k, k \in \{1, 2, 3\}$ , on its own. In the following, we exemplarily describe our approach for  $\varphi_3$  where we use a 3D copula  $C$  of the form

$$\varphi_3(x) = C(F_{M_1}(x_1), F_{M_2}(x_2), F_{M_{1 \wedge 2}}(x_3)). \quad (2.1)$$

Its corresponding density function is given by

$$c(u_1, u_2, u_3) = \frac{\partial^3}{\partial u_1 \partial u_2 \partial u_3} C(u_1, u_2, u_3), \quad (2.2)$$

where  $F_{M_1}$ ,  $F_{M_2}$  and  $F_{M_{1 \wedge 2}}$  denote the conditional marginal distribution functions of  $M_1$ ,  $M_2$  and  $M_{1 \wedge 2}$  given  $\{M_{1 \wedge 2} \neq 0\} \cap S^c$  and where  $u_1, u_2, u_3 \in [0, 1]$ . The cases  $\varphi_1$  and  $\varphi_2$  (note again that we use 2D copulas here, see Sections 3.1 and 3.2) can be treated analogously in two dimensions.

In order to obtain a parametric representation formula for  $\varphi_3$ , let  $\{(M_{1,i}, M_{2,i}, M_{1 \wedge 2,i})\}_{1 \leq i \leq n}$  be an i.i.d. sample of sample size  $n$ . Furthermore, assume that we have parametric models for the conditional marginal distribution and density functions  $F_{M_1}, f_{M_1}$  of  $M_1$  (with parameter  $\zeta_1$ ),  $F_{M_2}, f_{M_2}$  of  $M_2$  (with parameter  $\zeta_2$ ),  $F_{M_{1 \wedge 2}}$  and  $f_{M_{1 \wedge 2}}$  of  $M_{1 \wedge 2}$  (with parameter  $\zeta_3$ ), all conditioned on the event  $\{M_{1 \wedge 2} \neq 0\} \cap S^c$ . In particular, this means that we just consider the distribution and density functions of a subset of the total sample  $\{(M_{1,i}, M_{2,i}, M_{1 \wedge 2,i})\}_{1 \leq i \leq n}$ , fulfilling  $\{M_{1 \wedge 2} \neq 0\} \cap S^c$ . Let  $\mathcal{I}$  denote the set of all indexes  $i$  of this sample where  $\{M_{1 \wedge 2} \neq 0\} \cap S^c$ . Then, the cardinality of  $\mathcal{I}$  is  $n\hat{\rho}_3$ . Additionally, we assume parametric models for the 3D copula in (2.2) with parameter  $\zeta$ . Then, considering (2.1), the log-likelihood function is given by

$$\begin{aligned} & \log L(\zeta_1, \zeta_2, \zeta_3, \zeta) \\ &= \sum_{i \in \mathcal{I}} (\log f_{M_1}(M_{1,i}; \zeta_1) + \log f_{M_2}(M_{2,i}; \zeta_2) + \log f_{M_{1 \wedge 2}}(M_{1 \wedge 2,i}; \zeta_3) \\ & \quad + \log [c(F_{M_1}(M_{1,i}; \zeta_1), F_{M_2}(M_{2,i}; \zeta_2), F_{M_{1 \wedge 2}}(M_{1 \wedge 2,i}; \zeta_3); \zeta)]). \end{aligned} \quad (2.3)$$

Note that challenging numerical problems and time-consuming calculations occur when maximising the log-likelihood function (2.3) since all parameters are estimated at the same time. In order to prevent these difficulties, we proceed as in [20, 21] and optimise in two steps by first finding estimators for the parameters of the marginal densities and afterwards finding estimators for the copula function. This approach is called *pseudo-maximum-likelihood approach*. After having found estimators for the parameters of the marginal densities by the commonly used maximum-likelihood method, equation (2.3) can be simplified to

$$\text{pseudo log } L(\zeta) = \sum_{i \in \mathcal{I}} \log [c(\widehat{F}_{M_1}(M_{1,i}), \widehat{F}_{M_2}(M_{2,i}), \widehat{F}_{M_{1 \wedge 2}}(M_{1 \wedge 2,i}); \zeta)], \quad (2.4)$$

where  $\widehat{F}$  denotes the corresponding (conditional) empirical distribution function. Now, (2.4) can be utilised in order to fit the copula parameter  $\zeta$  to the data. An evaluation rule deciding which copula is the most suitable one among a given set of copulas is Akaike's information criterion and is defined as

$$2p - 2 \cdot \text{pseudo log } L(\widehat{\zeta}), \quad (2.5)$$

where  $p$  denotes the number of parameters in the model and  $\widehat{\zeta}$  is the corresponding maximum-likelihood estimator, see [20]. The smaller the value of (2.5) is, the better the copula fits our data.

### 3. RESULTS

We present now results and parametric formulas which are obtained by using the modelling approach of Section 2.2. In the following, we denote by  $\text{Naka}(r, s)$  the Nakagami distribution whose density is given by

$$f(x; r, s) = \frac{2r^r}{\Gamma(r)s^r} x^{2r-1} \exp\left(-\frac{r}{s}x^2\right),$$

where  $r, s, x > 0$ . Furthermore, we write  $\text{Wei}(k, \alpha)$  for the Weibull distribution with density function

$$f(x; k, \alpha) = \frac{k}{\alpha} \left(\frac{x}{\alpha}\right)^{k-1} \exp\left(-\left(\frac{x}{\alpha}\right)^k\right),$$

where  $k, \alpha, x > 0$ .

**3.1. Scenario I: Shortest paths from  $L_1$  and  $L_2$  to  $o$  do not intersect each other.** The goal in this part of the work is to find a suitable parametric approximation formula for  $\varphi_1$ , i.e., for the distribution of the random vector  $M$  under the condition that both paths  $p(o, L_1)$  and  $p(o, L_2)$  do not intersect each other except at the origin.

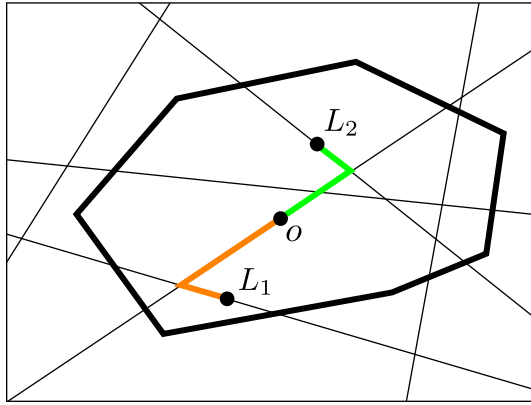


FIGURE 3.1. Scenario I: Shortest-paths from  $L_1$  (orange) respectively  $L_2$  (green) to  $o$  do not intersect each other except at  $o$

As  $p(o, L_1) \cap p(o, L_2) = \{o\}$ , we obtain  $M_1 = \nu_1(p(o, L_1))$ ,  $M_2 = \nu_1(p(o, L_2))$  and  $M_{1 \wedge 2} = 0$ , see Figure 3.1. Note that obviously  $M_1 \stackrel{\mathcal{D}}{=} M_2$ , as  $L_1$  and  $L_2$  are independently and uniformly distributed along  $S_H^*$ , where  $\stackrel{\mathcal{D}}{=}$  denotes equality in distribution.

**3.1.1. Marginal densities for scenario I.** For  $i \in \{1, 2\}$ , it turns out that  $M_i$  approximately follows a Nakagami distribution, i.e.  $M_i \sim \text{Naka}(r, s)$  with some shape parameter  $r$  and some spread parameter  $s$ . Note that the parameters  $r$  and  $s$  depend on the type of  $T$  as well as on the scaling parameter  $\kappa = \frac{\gamma}{\lambda_\epsilon}$ , see [26] for more information about this characteristic.

**3.1.2. Copula for scenario I.** In order to model the correlation structure between  $M_1$  and  $M_2$ , we decide to choose one of the following two-dimensional copulas: the elliptical ones of t-type and Gaussian type as well as the five Archimedean copulas Gumbel, Frank, Ali-Mikhail-Haq, Joe and Clayton. The reader is referred to [15] and [18] for more information about these well-known copulas. The copula which fits the data best according to (2.5) is of Gumbel type. In particular, we have the following representation

$$\text{Gumbel}_{\psi_1}(u_1, u_2) = \exp\left(-\left((-\log u_1)^{\psi_1} + (-\log u_2)^{\psi_1}\right)^{1/\psi_1}\right),$$

for some  $\psi_1 \geq 1$  and  $u_1, u_2 \in [0, 1]$ . Note that the type of the copula does neither depend on the underlying tessellation  $T$  nor on the scaling parameter  $\kappa$ . Furthermore, the copula parameter  $\psi_1$  depends only negligibly on  $\kappa$ . However, it moderately depends on the type of  $T$  so that more

precisely, we have  $\psi_1 = \psi_1(T)$ . In Section 4, the asymptotic distribution for the shortest-path tree  $G$  is given as  $\kappa \rightarrow \infty$ . It has a simple interpretation in terms of the underlying mathematical model and therefore we would be interested in investigating if this intuitive description is related to the choice of the Gumbel copula.

**3.2. Scenario II: Shortest-paths from  $L_1$  respectively  $L_2$  to  $o$  do intersect each other – one path is fully contained in the other one.** Next, we present a suitable parametric approximation formula for  $\varphi_2$ , i.e., for the distribution of the random vector  $M$  under the condition that both paths  $p(o, L_1)$  and  $p(o, L_2)$  do intersect each other not only in the origin but that one path is fully contained in the other one (see Figure 3.2).

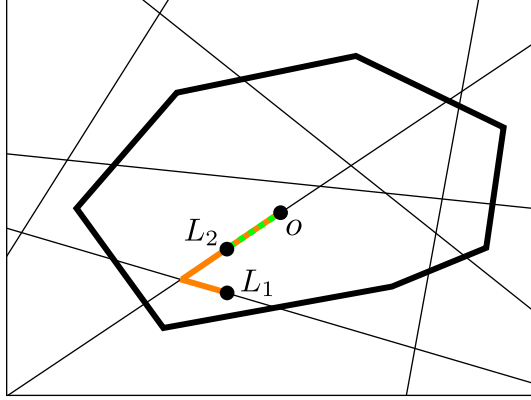


FIGURE 3.2. Scenario II: Shortest-paths from  $L_1$  (orange) respectively  $L_2$  (green) to  $o$  do intersect each other – green path is fully contained in the orange one

As

$$p(o, L_1) \cap p(o, L_2) = \begin{cases} p(o, L_2), & \text{if } p(o, L_2) \subset p(o, L_1) \\ p(o, L_1), & \text{if } p(o, L_1) \subset p(o, L_2) \end{cases},$$

we easily obtain

$$M_1 = \begin{cases} \nu_1(p(o, L_1) \setminus p(o, L_2)) > 0, & \text{if } p(o, L_2) \subset p(o, L_1) \\ 0, & \text{if } p(o, L_1) \subset p(o, L_2) \end{cases},$$

$$M_2 = \begin{cases} 0, & \text{if } p(o, L_2) \subset p(o, L_1) \\ \nu_1(p(o, L_2) \setminus p(o, L_1)) > 0, & \text{if } p(o, L_1) \subset p(o, L_2) \end{cases}$$

and furthermore

$$M_{1 \wedge 2} = \begin{cases} \nu_1(p(o, L_2)), & \text{if } p(o, L_2) \subset p(o, L_1) \\ \nu_1(p(o, L_1)), & \text{if } p(o, L_1) \subset p(o, L_2) \end{cases}.$$

**3.2.1. Marginal densities for scenario II.** When sampling  $S_H^*$  via Monte Carlo simulations and extracting  $M$ , we do not distinguish between  $L_1$  and  $L_2$  for reasons of comfort. As  $\mathbb{P}(M_i = 0 \mid \{M_{1 \wedge 2} \neq 0\} \cap S) = \frac{1}{2}$ , in our sample we have disturbing effects when considering the distribution of  $M_i, i \in \{1, 2\}$ . Therefore, we consider the random variable  $Z = \max\{M_1, M_2\}$ . It turns out that  $Z$  and  $M_{1 \wedge 2}$  approximately follow Weibull distributions, i.e.  $Z \sim \text{Wei}(k, \alpha)$  and  $M_{1 \wedge 2} \sim \text{Wei}(k', \alpha')$  with some shape parameters  $k, k' > 0$  and some scale parameters  $\alpha, \alpha' > 0$  which all depend on both the scaling parameter  $\kappa$  as well as on the type of the underlying tessellation  $T$ . In order to be able to provide a suitable parametric representation for the three-dimensional (conditional) distribution  $\varphi_2$  by means of  $Z$  and  $M_{1 \wedge 2}$ , one can put  $M_1 = \Omega Z$  and  $M_2 = (1 - \Omega)Z$ , where  $\Omega$  is a Bernoulli-distributed random variable with success probability  $\frac{1}{2}$ .

3.2.2. *Copula for scenario II.* The copulas which are taken into account for scenario II are the same as in Section 3.1.2. The one which fits the data best according to (2.5) is the Frank copula. In particular, we have the following representation

$$\text{Frank}_{\psi_2}(u_1, u_2) = -\frac{1}{\psi_2} \log \left( 1 + \frac{(\exp(-\psi_2 u_1) - 1)(\exp(-\psi_2 u_2) - 1)}{\exp(-\psi_2) - 1} \right),$$

for some  $\psi_2 > 0$  and  $u_1, u_2 \in [0, 1]$ . Since the correlation coefficient  $\text{cor}(M_{1 \wedge 2}, \max\{M_1, M_2\})$  of  $M_{1 \wedge 2}$  and  $\max\{M_1, M_2\}$  is negative, we transformed the data vector  $(M_{1 \wedge 2}, \max\{M_1, M_2\})$  into  $(-M_{1 \wedge 2}, \max\{M_1, M_2\})$  to be able to use more types of copulas. Clearly, this transformation has to be reversed when directly creating samples of  $M$ .

**3.3. Scenario III: Shortest-paths from  $L_1$  respectively  $L_2$  to  $o$  do intersect each other – both paths have a different subpath.** In this section, the goal is to find a suitable parametric approximation formula for  $\varphi_3$ , i.e., for the distribution of the random vector  $M$  under the condition that both paths  $p(o, L_1)$  and  $p(o, L_2)$  do intersect each other not only in the origin and that one path is not fully contained in the other one, see Figure 3.3.

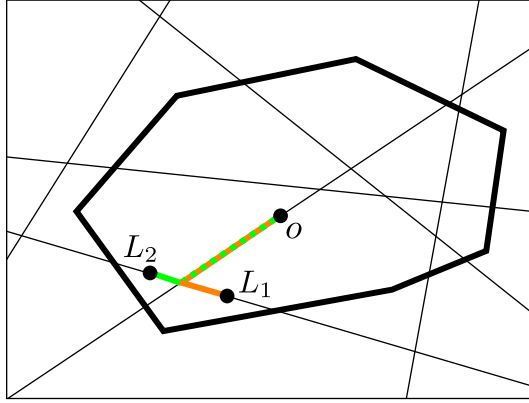


FIGURE 3.3. Scenario III: Shortest-paths from  $L_1$  (orange) respectively  $L_2$  (green) to  $o$  do intersect each other – both paths have a different subpath

3.3.1. *Marginal densities for scenario III.* Again, as in scenario I, we have  $M_1 \stackrel{\mathcal{D}}{=} M_2$ , since  $L_1$  and  $L_2$  are independently and uniformly distributed along  $S_H^*$ . In particular, we approximately have  $M_i \sim \text{Naka}(r', s')$  for some  $r' \geq 0.5$  and  $s' > 0$ . Besides, we approximately have  $M_{1 \wedge 2} \sim \text{Wei}(k'', \alpha'')$  for some  $k'', \alpha'' > 0$ . Note again that the parameters of the marginal densities depend both on the scaling parameter  $\kappa$  as well as on the type of the underlying tessellation  $T$ .

3.3.2. *Copula for scenario III.* In contrast to Sections 3.1.2 and 3.2.2 where two-dimensional Archimedean copulas of the form  $C(u_1, u_2) = \eta^{-1}(\eta(u_1) + \eta(u_2))$  with some generator  $\eta : [0, 1] \mapsto [0, \infty]$  were sufficient for representing  $\varphi_1$  and  $\varphi_2$ , we now have to go one step further and use three-dimensional copula functions in order to obtain a parametric formula for  $\varphi_3$ . A first approach could be the usage of three-dimensional Archimedean copulas of the form

$$C(u_1, u_2, u_3) = \eta^{-1}(\eta(u_1) + \eta(u_2) + \eta(u_3)), \quad (3.1)$$

where  $\eta : [0, 1] \mapsto [0, \infty]$  denotes the generator with some suitable parameter  $\tau$ . At first, similar to Section 3.2.2, some transformation of the extracted data is needed as some Archimedean copulas can only be used when positive correlation occurs. However, these three-dimensional Archimedean copulas with one generator  $\eta$  yet turn out to be not flexible enough for our data. In particular, we have

$$\begin{aligned} \text{cor}(F_{M_1}(M_1), F_{M_{1 \wedge 2}}(M_{1 \wedge 2})) &= \text{cor}(F_{M_2}(M_2), F_{M_{1 \wedge 2}}(M_{1 \wedge 2})) \\ &\neq \text{cor}(F_{M_1}(M_1), F_{M_2}(M_2)), \end{aligned}$$

which is incompatible with the symmetry of (3.1), since different correlation coefficients yield different parameters  $\tau$  which in turn cause different generators  $\eta$ .

To allow for asymmetries, a second possibility to pass from two to three dimensions is the usage of so-called nested Archimedean copulas with representation

$$C(u_1, u_2, u_3) = \eta_1^{-1}(\eta_1(\eta_2^{-1}(\eta_2(u_1) + \eta_2(u_2))) + \eta_1(u_3))$$

with generators  $\eta_1, \eta_2 : [0, 1] \mapsto [0, \infty]$  and suitable parameters  $\tau_1, \tau_2$ , see [12, 23]. However, a very uncomfortable problem of nesting Archimedean copulas into each other is the fact that the resulting structure is in general not a copula. In [12] and also [23], there are conditions under which such nested Archimedean copulas result in a copula structure, again. The simplest case of nesting two Archimedean copulas is nesting two Archimedean copulas of the same family, of course. Due to [23], for the Gumbel and the Clayton family, the resulting structure is a copula if the outer parameter  $\tau_1$  is less or equal than the inner parameter  $\tau_2$ . In [12], even further examples are provided. Unfortunately, for our data which was extracted from  $S_H^*$ , these copulas do not lead to satisfying results, either. The data is given in a way that the dependence structure (i.e. the absolute value of the correlation coefficient) between  $M_1$  and  $M_2$  is sometimes stronger and sometimes weaker than the one between  $M_{1 \wedge 2}$  and  $M_i$ , depending on  $\kappa$  and  $T$ . Note that it is reasonable that the correlation of  $M_1$  and  $M_2$  build the inner part of the nested copula as  $M_1 \stackrel{D}{=} M_2$ , so that the data should not be rearranged.

Nevertheless, as a third opportunity, we can take benefit from the three-dimensional elliptical copulas of t-type or Gaussian type and indeed, they turn out to provide fairly good results. According to (2.5), it turns out that the Gaussian copula fits to our data at least as good as (and sometimes even better than) the t-copula. This may at first seem counterintuitive, noticing that the Gaussian copula is a special case of the t-copula. However, after a second, closer look to the results, it becomes clear that the considered t-copula can be approximated by a Gaussian copula noticing that the respective degrees of freedom are sufficiently large. The latter one has less parameters which in turn causes – for almost equal values of the log-likelihood functions – smaller values of (2.5).

The Gaussian copula is given by

$$\text{Gauss}_{(\psi_3, \psi_4, \psi_5)}(u_1, u_2, u_3) = \Phi_\Sigma \left( \Phi^{-1}(u_1), \Phi^{-1}(u_2), \Phi^{-1}(u_3) \right), \quad (3.2)$$

where  $\Phi_\Sigma$  is the joint distribution function of a trivariate normal distribution with expectation vector zero and covariance matrix equal to the correlation matrix  $\Sigma$  which is given by

$$\Sigma = \begin{pmatrix} 1 & \psi_3 & \psi_4 \\ \psi_3 & 1 & \psi_5 \\ \psi_4 & \psi_5 & 1 \end{pmatrix}$$

and where  $\Phi^{-1}$  denotes the inverse of the distribution function of a standard normal distributed random variable. Note that  $\psi_4 = \psi_5$  and that the copula only depends on the correlation coefficient vector  $\psi = (\psi_3, \psi_4)$  which in turn depends on  $\kappa$  and the type of  $T$ . In particular, according to the choice of  $\kappa$  and  $T$ , we have  $\psi_3 \in [0.15, 0.30]$  and  $\psi_4 \in [-0.35, -0.10]$ .

**3.4. Model validation.** In order to validate the three-dimensional model provided in the present paper, we help ourselves by using the multivariate Wald-Wolfowitz two-sample test [9] which we already had successfully applied in two dimensions within another framework, see [21]. In particular, due to the fact that this test can be used in arbitrary dimensions  $d \geq 2$  and since it is of increasing difficulty to visually compare two data sets in higher dimensions, the Wald-Wolfowitz two-sample test is one suitable statistical tool to validate our data in a formally correct, mathematical way. For the convenience of the reader, we shortly summarise the general settings of the test. Denote by  $X_1, \dots, X_n, Y_1, \dots, Y_m \in \mathbb{R}^3$  independent trivariate vectors and let furthermore  $X_1, \dots, X_n \sim F_X$  and  $Y_1, \dots, Y_m \sim F_Y$  for some arbitrary distribution functions  $F_X$  and  $F_Y$ . The null-hypothesis of the test is given by  $H_0 : F_X = F_Y$ , the alternative hypothesis by  $H_1 : F_X \neq F_Y$ . Let  $S$  denote the number of disjoint subtrees resulting from erasing

all edges of the minimal spanning tree (it is based on the joint sample  $X_1, \dots, X_n, Y_1, \dots, Y_m$ ) with nodes from different samples. Besides, let  $D$  denote the number of edge pairs that share a common node in this minimal spanning tree. Then, the test statistic  $T_{\text{WW}}$  is given by

$$T_{\text{WW}} = \frac{S - \mathbb{E}S}{\sqrt{\text{Var}(S|D)}},$$

where  $\text{Var}(S|D) = \mathbb{E}(S^2|D) - (\mathbb{E}(S|D))^2$ . In [9], it is stated that under  $H_0$ ,  $T_{\text{WW}}$  is asymptotically  $N(0, 1)$ -distributed and therefore,  $H_0$  is rejected if

$$|T_{\text{WW}}| > z_{1-\alpha/2},$$

where  $z_{1-\alpha/2}$  denotes the  $1 - \alpha/2$ -quantile of the standard normal distribution.

In the following, we provide test results for various constellations of the underlying tessellation  $T$  and the scaling parameter  $\kappa$  for scenarios I, II and III. Note that in scenario II, we consider without loss of generality  $M_2 = 0$ . Figure 3.4 displays on the left-hand side the data points extracted out of  $S_H^*$  for scenario I (green) and scenario II (red), considering an underlying PDT with scaling parameter  $\kappa = 120$ . On the right-hand side, data points by directly sampling from the fitted parametric copulas and marginal distributions are shown. The reader can observe that both scatterplots match quite well.

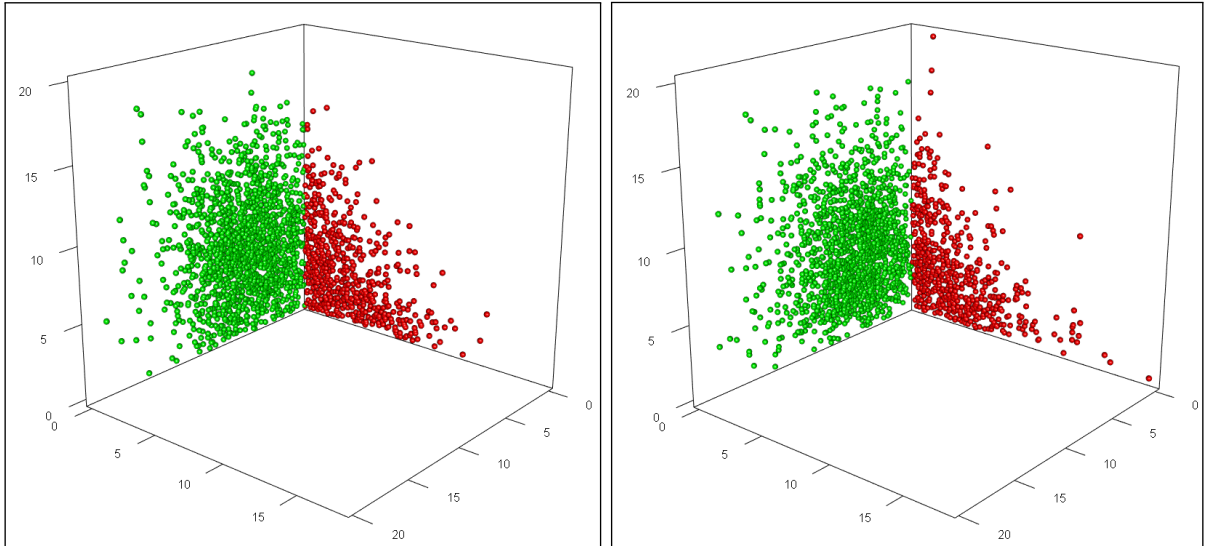


FIGURE 3.4. 2D-scatterplots of scenario I (green) and II (red) data points, extracted from  $S_H^*$  with PDT,  $\kappa = 120$  (left) and directly sampled from the copula model (right)

Table 3.1 shows results of the Wald-Wolfowitz two-sample test in scenario I on the left-hand side and scenario II on the right-hand side for various constellations of  $T$  and  $\kappa$ . In each case, the null hypothesis  $H_0$  is clearly *not* rejected since the values of  $|T_{\text{WW}}|$  are always smaller than  $z_{0.975} = 1.96$ . Note that the power of the test used in this context is unfortunately not very high. However, since alternatives are rather barely available for vectorial datasets, we nevertheless make use of it.

Figure 3.5 displays on the left-hand side the data points extracted out of  $S_H^*$  for scenario III, again considering an underlying PDT with scaling parameter  $\kappa = 120$ . On the right-hand side, data points obtained by directly sampling from the fitted parametric copulas and marginal distributions are shown. Again, the reader can observe that both scatterplots match quite well.

In Table 3.2, the reader can observe results of the Wald-Wolfowitz two-sample test for various constellations of  $T$  and  $\kappa$ . Again, in each case, the null hypothesis  $H_0$  is clearly *not* rejected.

TABLE 3.1. Results of Wald-Wolfowitz test for scenarios I (left) and II (right)

$T$	$\kappa$	$ T_{\text{WW}} $	$T$	$\kappa$	$ T_{\text{WW}} $
PVT	20	0.0779	PVT	20	0.0766
PVT	625	0.0716	PVT	625	0.0694
PDT	40	0.0176	PDT	40	0.0621
PDT	120	0.0788	PDT	120	0.0317
PLT	90	0.0137	PLT	90	0.1156
PLT	825	0.0190	PLT	825	0.0863

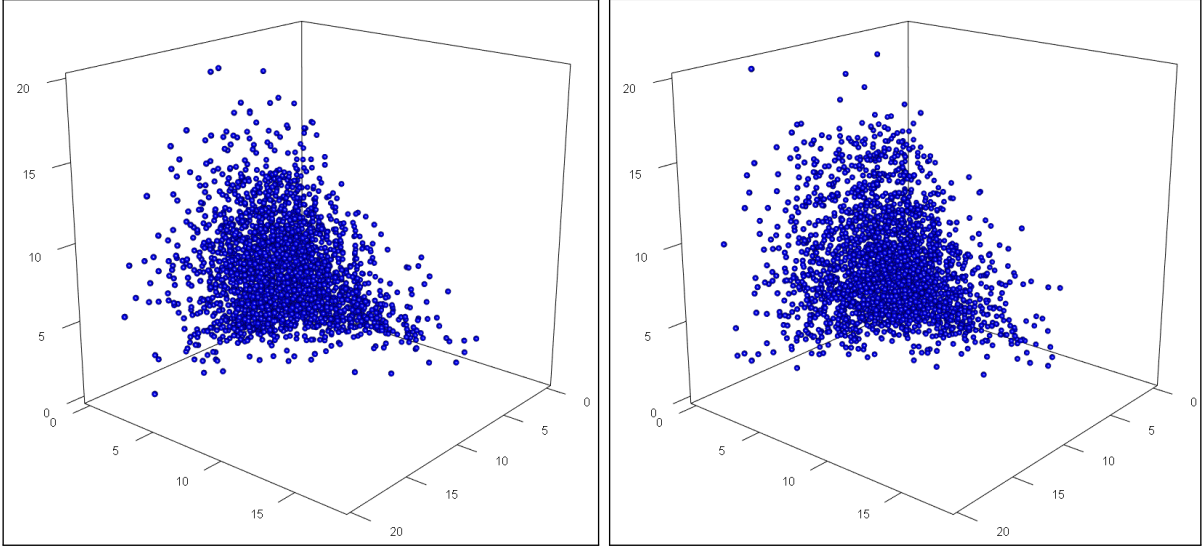


FIGURE 3.5. 3D-scatterplots of scenario III data points, extracted from  $S_H^*$  with PDT,  $\kappa = 120$  (left) and directly sampled from the copula model (right)

TABLE 3.2. Results of Wald-Wolfowitz test for scenario III

$T$	$\kappa$	$ T_{\text{WW}} $
PVT	20	0.0045
PVT	625	0.0320
PDT	40	0.0490
PDT	120	0.0541
PLT	90	0.0172
PLT	825	0.0674

Finally, Figure 3.6 displays on the left-hand side data points extracted out of  $S_H^*$ , again considering an underlying PDT with scaling parameter  $\kappa = 120$ . Besides, on the right-hand side, the corresponding directly sampled data points are shown.

Summarising the validation obtained by Figures 3.4, 3.5 and 3.6 as well as Tables 3.1 and 3.2, we can state that the suggested modelling approach in the present paper for a direct sampling of shortest-path trees in sparse LLC networks seems to be adequate.

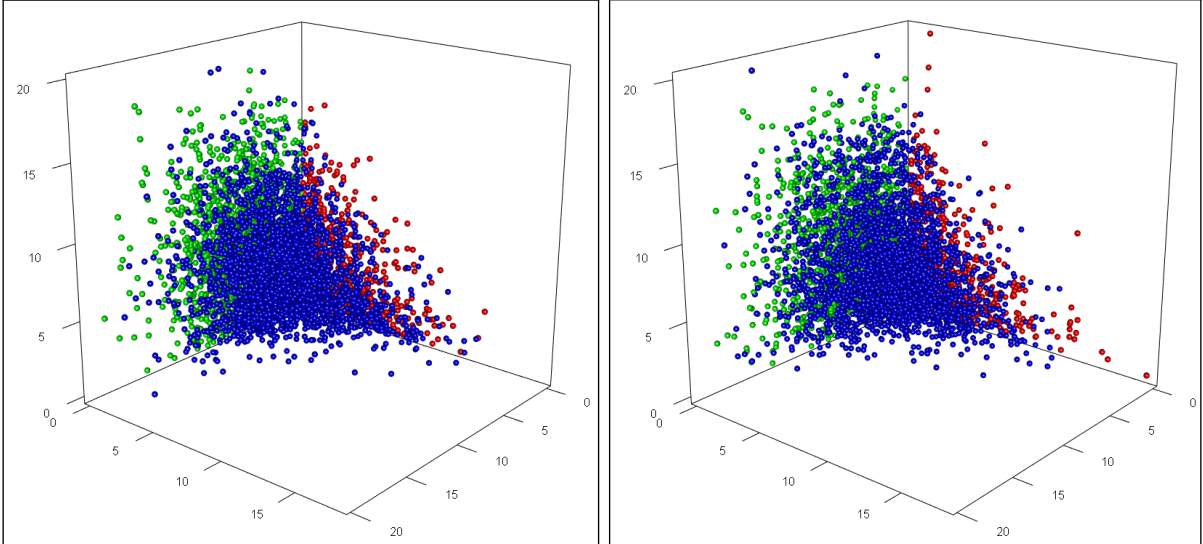


FIGURE 3.6. 3D-scatterplots of scenario I (green), scenario II (red) and scenario III (blue) data points, extracted from  $S_H^*$  with PDT,  $\kappa = 120$  (left) and directly sampled from the copula model (right)

#### 4. A LIMIT THEOREM FOR SHORTEST-PATH TREES

The parametric copula approach proposed in this paper for directly simulating shortest-path trees in sparse LLC networks turns out to be a suitable, powerful and quick sampling possibility if the scaling parameter  $\kappa$  is neither too small nor too large, i.e.  $\kappa \in [10, 1000]$ . However, one may ask if a validation of the approach is still possible for other values of  $\kappa$ , e.g. as  $\kappa \rightarrow \infty$ . Indeed, in this case Monte Carlo simulations become more and more time-consuming and beyond a certain threshold for  $\kappa$ , it is not reasonable to proceed in such a way. Therefore, we provide a limit distribution for the shortest-path tree if  $\kappa \rightarrow \infty$ . In the following, we assume that  $\gamma$  is fixed and let  $\lambda_\ell \rightarrow 0$ .

For the investigation of the asymptotic scenario as  $\lambda_\ell \rightarrow 0$ , it is helpful to make the dependence on  $\lambda_\ell$  explicit in the notation of relevant quantities. In particular, we write  $L_{i,\lambda_\ell}, M_{i,\lambda_\ell}, M_{1\wedge 2,\lambda_\ell}, X_{H,\lambda_\ell}$  and  $\Xi_{H,\lambda_\ell}^*$  instead of  $L_i, M_i, M_{1\wedge 2}, X_H$  and  $\Xi_H^*$ , respectively. For  $i \in \{1, 2\}$ , we write  $M'_{i,\lambda_\ell} = M_{i,\lambda_\ell} + M_{1\wedge 2,\lambda_\ell} = \nu_1(p(o, L_{i,\lambda_\ell}))$  for the length of the shortest path from the  $i$ -th subscriber to the root. Note that as  $\lambda_\ell \rightarrow 0$ , the contribution of  $M_{1\wedge 2,\lambda_\ell}$  to  $M'_{i,\lambda_\ell}$  becomes negligible. Therefore, knowing the asymptotic behaviour of  $(M'_{1,\lambda_\ell}, M'_{2,\lambda_\ell})$  is sufficient for describing the asymptotic shortest-path tree associated with two LLC. Finally, the asymptotic behaviour of an appropriately scaled version of the random vector  $(M'_{1,\lambda_\ell}, M'_{2,\lambda_\ell})$  can be described as follows. For  $i \in \{1, 2\}$ , consider the random variable  $M'_i = \xi |L'_i|$  where  $\xi$  is the so-called time constant appearing in [26, Theorem 3.2]. Furthermore, the random vectors  $L'_1, L'_2$  are independent and conditionally uniformly distributed in  $\Xi^*$  given  $\Xi^*$ , where  $\Xi^*$  denotes the typical Poisson-Voronoi cell induced by a Poisson point process with intensity  $\gamma$ . This uniform distribution is due to two intuitive facts. First, as  $\lambda_\ell$  tends to 0, the scaled typical serving zone  $\sqrt{\lambda_\ell} \Xi_{H,\lambda_\ell}^*$  converges in distribution to the typical Poisson-Voronoi cell  $\Xi^*$ . Second, the scaled road system  $\sqrt{\lambda_\ell} T^{*,(1)}$  gets infinitely dense, so that LLC are located in the whole cell.

**Theorem 4.1.** *As  $\lambda_\ell \rightarrow 0$ , the random vector  $(\sqrt{\lambda_\ell} M'_{1,\lambda_\ell}, \sqrt{\lambda_\ell} M'_{2,\lambda_\ell})$  converges to  $(M'_1, M'_2)$  in distribution.*

In order to prove Theorem 4.1, we first recall from [26] that  $\sqrt{\lambda_\ell}(M'_{i,\lambda_\ell} - \xi |L'_{i,\lambda_\ell}|)$  for  $i \in \{1, 2\}$  tends to 0 in probability as  $\lambda_\ell \rightarrow 0$ . Therefore, it remains to determine the asymptotic behaviour

of the bivariate random vector

$$(\sqrt{\lambda_\ell}|L_{1,\lambda_\ell}|, \sqrt{\lambda_\ell}|L_{2,\lambda_\ell}|).$$

Our first goal is to show that the random vector  $(\sqrt{\lambda_\ell}L_{1,\lambda_\ell}, \sqrt{\lambda_\ell}L_{2,\lambda_\ell})$  converges in distribution to  $(L'_1, L'_2)$  consisting of two independent random variables  $L'_1, L'_2$  which are conditionally uniformly distributed inside the typical Poisson-Voronoi cell  $\Xi^*$ , given  $\Xi^*$ . To prove this claim, we proceed in two steps. First, we show that using a suitable coupling,  $(\sqrt{\lambda_\ell}L_{1,\lambda_\ell}, \sqrt{\lambda_\ell}L_{2,\lambda_\ell})$  is asymptotically equivalent with  $(\sqrt{\lambda_\ell}L''_{1,\lambda_\ell}, \sqrt{\lambda_\ell}L''_{2,\lambda_\ell})$ , where conditioned on  $T^*$  and  $\Xi_{H,\lambda_\ell}^*$ , the random variables  $L''_{1,\lambda_\ell}, L''_{2,\lambda_\ell}$  are independent and uniformly distributed in  $\Xi_{H,\lambda_\ell}^*$ . Then, in the second step, we show that using a further suitable coupling,  $(\sqrt{\lambda_\ell}L''_{1,\lambda_\ell}, \sqrt{\lambda_\ell}L''_{2,\lambda_\ell})$  is asymptotically equivalent with  $(L'_1, L'_2)$ . To make this more precise, we use the following two auxiliary results which are proven in Appendix B.

**Lemma 4.2.** *There exists a common probability space  $(\Omega, \mathcal{F}, \mathbb{P})$  on which  $(L_{1,\lambda_\ell}, L_{2,\lambda_\ell})$  and  $(L''_{1,\lambda_\ell}, L''_{2,\lambda_\ell})$  are given such that for every  $i \in \{1, 2\}$  and  $\varepsilon > 0$ ,*

$$\lim_{\lambda_\ell \rightarrow 0} \mathbb{P}(\sqrt{\lambda_\ell}|L_{i,\lambda_\ell} - L''_{i,\lambda_\ell}| \geq \varepsilon) = 0.$$

**Lemma 4.3.** *There exists a common probability space  $(\Omega, \mathcal{F}, \mathbb{P})$  on which  $(L'_1, L'_2)$  and  $(L''_{1,\lambda_\ell}, L''_{2,\lambda_\ell})$  are given such that for every  $i \in \{1, 2\}$  and  $\varepsilon > 0$ ,*

$$\lim_{\lambda_\ell \rightarrow 0} \mathbb{P}(|L'_i - \sqrt{\lambda_\ell}L''_{i,\lambda_\ell}| \geq \varepsilon) = 0.$$

Using Lemmas 4.2 and 4.3, the proof of Theorem 4.1 is now straightforward.

*Proof of Theorem 4.1.* As mentioned above, for  $i \in \{1, 2\}$ , the scaled difference  $\sqrt{\lambda_\ell}(M'_{i,\lambda_\ell} - \xi|L_{i,\lambda_\ell}|)$  tends to 0 in probability as  $\lambda_\ell \rightarrow 0$ . Moreover, Lemmas 4.2 and 4.3 imply that  $\sqrt{\lambda_\ell}|L_{i,\lambda_\ell}| - |L'_i|$  tends to 0 in probability as  $\lambda_\ell \rightarrow 0$ , where again  $i \in \{1, 2\}$  is arbitrary. Combining these observations shows that for every  $i \in \{1, 2\}$  the random variable  $\sqrt{\lambda_\ell}M'_{i,\lambda_\ell}$  converges to  $M'_i$  in probability as  $\lambda_\ell \rightarrow 0$ .  $\square$

## 5. CONCLUSIONS AND OUTLOOK

In the present paper, we provide a three-dimensional, parametric copula approach to fully describe the distribution of shortest-path trees in sparse LLC networks with two LLC. In particular, knowing the distribution of the random vector  $M = (M_1, M_2, M_{1 \wedge 2})$  is sufficient to achieve this goal. Its distribution function  $F_M(x)$  can be represented as a mixture  $\rho_1 \cdot \varphi_1(x) + \rho_2 \cdot \varphi_2(x) + \rho_3 \cdot \varphi_3(x)$  of the three conditional distributions  $\varphi_1(x), \varphi_2(x)$  and  $\varphi_3(x)$  with mixing probabilities  $\rho_1 = \mathbb{P}(M_{1 \wedge 2} = 0)$ ,  $\rho_2 = \mathbb{P}((M_{1 \wedge 2} \neq 0) \cap S)$  and  $\rho_3 = \mathbb{P}((M_{1 \wedge 2} \neq 0) \cap S^c)$ . Each trivariate distribution function  $\varphi_i, i \in \{1, 2, 3\}$ , is approximated by a suitable parametric copula function combining the corresponding parametric marginal distribution functions. More precisely, for  $\varphi_1$ , we have a Gumbel copula combining Nakagami-distributed marginals. Additionally, for  $\varphi_2$ , a Frank copula adds the correlation structure to the corresponding Weibull-distributed marginals, whereas for  $\varphi_3$ , a Gaussian copula joins the corresponding Nakagami- and Weibull-distributed marginals. Visual validation together with the multivariate Wald-Wolfowitz test proved our modelling approach to be suitable. Finally, we provided a limit theorem for the asymptotic behaviour of the shortest-path tree  $G$  as the linear intensity  $\lambda_\ell$  of the HLC tends to 0.

A possibility for prospective work is the extension of sparse LLC networks to three or even more LLC. Note that with increasing number of LLC, the number of possible scenarios concerning joint shortest subpaths to the corresponding HLC, equal or different directions of incoming paths into HLC, etc. also increases. This can be very cumbersome for a moderately large number of LLC. Besides, one could extend the types of models representing the underlying infrastructure by replacing PVT, PDT and PLT, respectively, by other random geometric graphs such as STIT-tessellations,  $\beta$ -skeletons, etc. see e.g. [1, 5, 16, 25]. In Section 3, it was shown the type of the optimal copula in each of the considered network scenarios does not depend on

the choice of the underlying tessellation. Therefore, it would be interesting to investigate if this universality is related to the simple mathematical description of the asymptotic distribution of the shortest-path tree stated in Theorem 4.1.

#### ACKNOWLEDGEMENTS

This work was supported by Orange Labs through Research Grant No. 46146063-9241. The authors would like to thank the referee for his/her thorough review of the manuscript. His/her comments helped to substantially improve the paper.

#### APPENDIX A. SOME PRELIMINARY RESULTS

In order to prove Lemmas 4.2 and 4.3, we first derive some preliminary results that may also be of independent interest. On the one hand, we show that the length of the segment system  $T^{*,(1)}$  in large sampling windows concentrates around its expected value. To be more precise, Lemma A.3 provides a stretched-exponential concentration result corresponding to large deviations of the segment lengths. On the other hand, we show that asymptotically, the typical Cox-Voronoi cell  $\Xi_{H,\lambda_\ell}^*$  approaches a typical Poisson-Voronoi cell, which is independent of  $T^*$ . This is achieved by using a coupling construction, which is presented in Lemma A.5.

**A.1. Concentration result for large deviations of total edge lengths.** In this subsection, we present a stretched-exponential large-deviation estimate for the total length  $\nu_1(T^{(1)} \cap Q_s(o))$ , where  $Q_s(o) = [-s/2, s/2]^2$  denotes the square of side length  $s$  centered at  $o$ . As this concentration result seems not to be covered by the existing approaches in stochastic geometry (see e.g. [4, 8]), it may be of interest to note that our proof generalises also to dimensions larger than 2. We say that a  $[1, \infty)$ -indexed family of events  $\{A_s\}_{s \geq 1}$  occur *with high probability* (whp) if

$$\liminf_{s \rightarrow \infty} \frac{\log(-\log(1 - \mathbb{P}(A_s)))}{\log s} > 0. \quad (\text{A.1})$$

Similarly, we say that a sequence of events  $\{A_n\}_{n \in \{1, 2, \dots\}}$  occur *with high probability* (whp) if

$$\liminf_{n \rightarrow \infty} \frac{\log(-\log(1 - \mathbb{P}(A_n)))}{\log n} > 0. \quad (\text{A.2})$$

The following concentration result is particularly useful for our purposes.

**Lemma A.1.** *Let  $\varepsilon > 0$  and let  $\{Y_n\}_{n \geq 1}$  be a sequence of i.i.d. non-negative random variables such that  $Y_1$  has a finite stretched-exponential moment, i.e., there exists  $\alpha \in (0, 1)$  with  $\mathbb{E}\exp(Y_1^\alpha) < \infty$ . Then, for  $n \geq 1$ , the events*

$$\left| \sum_{i=1}^n Y_i - n\mathbb{E}Y_1 \right| \leq n\varepsilon \quad (\text{A.3})$$

*occur whp.*

Note that the statement of Lemma A.1 is a special case of a stretched exponential concentration result due to J. V. Linnik and we refer the reader to the original paper [14, Theorem 2] for details.

In order to derive a concentration result for large deviations of the total edge length in a finite sampling window, it is convenient to consider graphs that satisfy a suitable stabilisation condition. To be more precise, in the following  $g : \mathbb{N} \rightarrow \mathbb{T}$  is a measurable motion-covariant mapping, where  $\mathbb{N}$  denotes the family of all locally finite subsets of  $\mathbb{R}^2$  endowed with the smallest  $\sigma$ -algebra  $\mathcal{N}$  that contains all open sets of the Fell topology on  $\mathbb{N}$ , see [24]. As in [10], in the present setting we require the existence of a suitable radius of stabilisation. Let  $X$  be a stationary,  $m$ -dependent point process in  $\mathbb{R}^2$ . Putting  $\mathbb{Z}_{+, \infty} = \{1, 2, \dots\} \cup \{\infty\}$ , in the present setting, a radius of stabilisation is defined to be an  $\mathcal{N}$ -measurable function  $b : \mathbb{N} \rightarrow \mathbb{Z}_{+, \infty}$  such that with probability 1, it holds that

$$g(X) \cap Q_1(o) = g((X \cap Q_{b(X)}(o)) \cup \psi) \cap Q_1(o) \quad (\text{A.4})$$

for all locally finite  $\psi \subset \mathbb{R}^2 \setminus Q_{b(X)}(o)$ , and that

$$\min\{b(X), n + 1\} = \min\{b(X \cap Q_n(o) \cup \psi), n + 1\}, \quad (\text{A.5})$$

for all  $n \in [1, \infty) \cap \mathbb{Z}$  and locally finite  $\psi \subset \mathbb{R}^2 \setminus Q_n(o)$ . Then, we require that

**(T)** the events  $\{b(X) \leq s\} \cap \{\nu_1(g(X) \cap Q_1(o)) \leq s\}$  occur whp.

Using these preliminaries, we now prove the desired stretched-exponential large-deviation result for  $\nu_1(T^{(1)} \cap Q_s(o))$ .

**Lemma A.2.** *Let  $\varepsilon > 0$  and  $X$  be a stationary,  $m$ -dependent point process in  $\mathbb{R}^2$ . Let  $g : \mathbb{N} \rightarrow \mathbb{T}$  be an  $\mathcal{N}$ -measurable and motion-covariant mapping such that  $T = g(X)$  satisfies condition **(T)**. Then, for  $s \geq 1$  the events  $|\nu_1(T^{(1)} \cap Q_s(o)) - \gamma s^2| \leq \varepsilon s^2$  occur whp.*

*Proof.* Our idea of proof is based on a Bernstein-type approach, see [17]. We only prove the assertion on upper large deviations and note that the claim for lower large deviations can be obtained similarly. First, put  $s_1 = \lceil 8\sqrt{s} \rceil$  and  $s_2 = \lceil s/s_1 \rceil s_1$ . Subdivide  $Q_{s_2}(o)$  into  $k_1 = (s_2/s_1)^2$  congruent sub-squares  $Q'_1, \dots, Q'_{k_1}$  of side length  $s_1$ . Next, further subdivide each  $Q'_i$  into  $k_2 = s_1^2$  congruent sub-squares  $Q_{i,1}, \dots, Q_{i,k_2}$  of side length 1 and write  $x_{i,j}$  for the centre of the square  $Q_{i,j}$ , see Figure A.1.

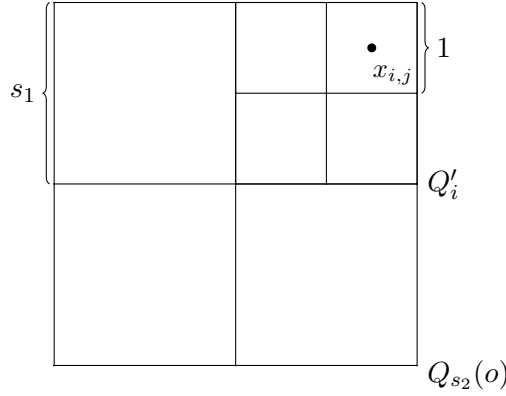


FIGURE A.1. Subdivision of  $Q_{s_2}(o)$

Observe that by choosing an appropriate indexing, we can partition the set of sub-squares  $\{Q_{i,j}\}_{\substack{1 \leq i \leq k_1 \\ 1 \leq j \leq k_2}}$  into  $k_2$  families

$$\{Q_{1,1}, Q_{2,1}, \dots, Q_{k_1,1}\}, \dots, \{Q_{1,k_2}, Q_{2,k_2}, \dots, Q_{k_1,k_2}\},$$

such that  $|x_{i_1,j} - x_{i_2,j}| \geq s_1$  for all  $j \in \{1, \dots, k_2\}$  and all  $i_1, i_2 \in \{1, \dots, k_1\}$  with  $i_1 \neq i_2$ . If  $\nu_1(T^{(1)} \cap Q_s(o)) \geq (\gamma + \varepsilon)s^2$ , then  $\sum_{i=1}^{k_1} \nu_1(T^{(1)} \cap Q_{i,j_0}) \geq (\gamma + \varepsilon)s^2/k_2$  for some  $j_0 \in \{1, \dots, k_2\}$ . Because of

$$\mathbb{P}\left(\bigcup_{j_0=1}^{k_2} \left\{ \sum_{i=1}^{k_1} \nu_1(T^{(1)} \cap Q_{i,j_0}) \geq (\gamma + \varepsilon)s^2/k_2 \right\}\right) \leq k_2 \mathbb{P}\left(\sum_{i=1}^{k_1} \nu_1(T^{(1)} \cap Q_{i,1}) \geq (\gamma + \varepsilon)s^2/k_2\right),$$

it suffices to consider the case  $j_0 = 1$ . Putting

$$C_s^{(1)} = \{g(X \cap Q_{3\sqrt{s}}(x_{1,1})) \cap Q_{1,1} = g(X) \cap Q_{1,1}\},$$

we conclude from condition **(T)** that the events  $\{C_s^{(1)}\}_{s \geq 1}$  occur whp. Write  $U_i = \nu_1(g(X) \cap Q_{i,1})$ ,  $V_i = \nu_1(g(X \cap Q_{3\sqrt{s}}(x_{i,1})) \cap Q_{i,1})$  and observe that by stationarity, the marginal distribution of  $U_i$  does not depend on  $i$  or  $s$ . Also note that the random variables  $V_1, \dots, V_{k_1}$  are

i.i.d. Finally, for  $i \in \{1, \dots, k_1\}$  we put  $W_i = \nu_1(g(X^{(i)}) \cap Q_{i,1})$ , where  $X^{(1)}, \dots, X^{(k_1)}$  are independent copies of  $X$ . Then,

$$\begin{aligned} \mathbb{P}\left(\sum_{i=1}^{k_1} U_i \geq (\gamma + \varepsilon)s^2/k_2\right) &\leq k_1(1 - \mathbb{P}(C_s^{(1)})) + \mathbb{P}\left(\sum_{i=1}^{k_1} V_i \geq (\gamma + \varepsilon)s^2/k_2\right) \\ &\leq 2k_1(1 - \mathbb{P}(C_s^{(1)})) + \mathbb{P}\left(\sum_{i=1}^{k_1} W_i \geq (\gamma + \varepsilon/2)k_1\right), \end{aligned}$$

provided that  $s \geq 1$  is sufficiently large. Since  $k_1 \geq s^{1/4}$  for all sufficiently large  $s \geq 1$ , an application of Lemma A.1 completes the proof.  $\square$

**Remarks.** It is not difficult to prove a large-deviation result for the case of the isotropic Poisson line tessellation directly. Furthermore, for the Poisson-Delaunay tessellation and Poisson-Voronoi tessellation, it is shown in [10] that the conditions of Lemma A.2 are satisfied.

Next, we observe that we may pass from  $\nu_1(T^{(1)} \cap Q_s(o))$  to  $\nu_1(T^{*,(1)} \cap Q_s(o))$ .

**Lemma A.3.** *Suppose that for every  $\varepsilon > 0$  it holds that the events  $|\nu_1(T^{(1)} \cap Q_s(o)) - \gamma s^2| \leq \varepsilon s^2$  occur whp. Then, for every  $\varepsilon > 0$ ,*

$$\liminf_{s \rightarrow \infty} \frac{\log\left(-\log\left(\sup_{x \in \mathbb{R}^2} \mathbb{P}(|\nu_1(T^{*,(1)} \cap Q_s(x)) - \gamma s^2| \geq \varepsilon s^2)\right)\right)}{\log s} > 0. \quad (\text{A.6})$$

*Proof.* Indeed, for all sufficiently large  $s > 0$  the Cauchy-Schwarz inequality yields

$$\begin{aligned} \mathbb{P}(\nu_1(T^{*,(1)} \cap Q_s(x)) \geq \gamma s^2 + \varepsilon s^2) &= \gamma^{-1} \mathbb{E} \int_{T \cap Q_1(o)} 1_{\nu_1(T^{(1)} \cap Q_s(x+y)) \geq (\gamma + \varepsilon)s^2} dy \\ &\leq \gamma^{-1} \mathbb{E} \int_{T \cap Q_1(o)} 1_{\nu_1(T^{(1)} \cap Q_{s+2}(x)) \geq (\gamma + \varepsilon/2)(s+2)^2} dy \\ &= \gamma^{-1} \mathbb{E} \nu_1(T^{(1)} \cap Q_1(o)) 1_{\nu_1(T^{(1)} \cap Q_{s+2}(x)) \geq (\gamma + \varepsilon/2)(s+2)^2} \\ &\leq \gamma^{-1} (\mathbb{E} \nu_1(T^{(1)} \cap Q_1(o))^2)^{1/2} \mathbb{P}(\nu_1(T^{(1)} \cap Q_{s+2}(x)) \geq (\gamma + \varepsilon/2)(s+2)^2)^{1/2} \\ &= \gamma^{-1} (\mathbb{E} \nu_1(T^{(1)} \cap Q_1(o))^2)^{1/2} \mathbb{P}(\nu_1(T^{(1)} \cap Q_{s+2}(o)) \geq (\gamma + \varepsilon/2)(s+2)^2)^{1/2}. \end{aligned}$$

Using an analogous computation for deviations in the other direction proves Lemma A.3.  $\square$

**A.2. Asymptotic independence of  $T^*$  and the Cox-Voronoi cell.** A key step in the derivation of the asymptotic behavior of  $(\sqrt{\lambda_\ell} M'_{1,\lambda_\ell}, \sqrt{\lambda_\ell} M'_{2,\lambda_\ell})$  is the asymptotic independence of  $T^*$  and the zero-cell in the Voronoi tessellation based on  $X_{H,\lambda_\ell} \cup \{o\}$ . Recall that we assume that  $T$  is a Poisson-Delaunay tessellation, Poisson-Voronoi tessellation or a Poisson line tessellation. First, we show that there is a good chance that the Cox-Voronoi cell at the origin contains a given small square and is contained in a given large square. Recall that  $X_{H,\lambda_\ell}$  denotes a Cox process on  $T^*$  with linear intensity  $\lambda_\ell > 0$  and  $\Xi_{H,\lambda_\ell}^*$  is the zero-cell of the Voronoi tessellation based on  $X_{H,\lambda_\ell} \cup \{o\}$ . For  $\lambda_\ell > 0$  and  $r > 1$  put

$$E_{r,\lambda_\ell}^{(1)} = \{Q_{1/r}(o) \subset \sqrt{\lambda_\ell} \Xi_{H,\lambda_\ell}^* \subset Q_r(o)\}^c.$$

In the following,  $B_r(x) = \{y \in \mathbb{R}^2 : |y - x| \leq r\}$  denotes the disk with radius  $r > 0$  centered at  $x \in \mathbb{R}^2$ .

**Lemma A.4.** *It holds that  $\lim_{r \rightarrow \infty} \limsup_{\lambda_\ell \rightarrow 0} \mathbb{P}(E_{r,\lambda_\ell}^{(1)}) = 0$ .*

*Proof.* Subdivide  $Q_{r\lambda_\ell^{-1/2}}(o)$  into 25 congruent sub-squares  $Q_{\lambda_\ell,1}, \dots, Q_{\lambda_\ell,25}$  of side length  $r\lambda_\ell^{-1/2}/5$  such that  $\text{int } Q_{\lambda_\ell,i} \cap \text{int } Q_{\lambda_\ell,j} = \emptyset$  if  $i \neq j$ , where  $\text{int } Q_{\lambda_\ell,i}$  denotes the topological interior

of  $Q_{\lambda_\ell, i}$ . Then, it is easy to check that the event  $\{\Xi_{H, \lambda_\ell}^* \not\subset Q_{r\lambda_\ell^{-1/2}}(o)\}$  cannot occur if  $\min_{i \in \{1, \dots, 25\}} \#(X_{H, \lambda_\ell} \cap Q_{\lambda_\ell, i}) \geq 1$ , where  $\#$  denotes cardinality. Observe that by Lemma A.3,

$$\lim_{\lambda_\ell \rightarrow 0} \mathbb{P}\left(\min_{i \in \{1, \dots, 25\}} \nu_1(T^{*,(1)} \cap Q_{\lambda_\ell, i}) \leq \gamma r^2 \lambda_\ell^{-1} / 50\right) = 0.$$

Furthermore, if  $N_\mu$  denotes a Poissonian random variable with expectation  $\mu > 0$ , then

$$\lim_{r \rightarrow \infty} \sup_{\mu \geq \gamma r^2 / 50} \mathbb{P}(N_\mu = 0) = 0,$$

so that  $\lim_{r \rightarrow \infty} \limsup_{\lambda_\ell \rightarrow 0} \mathbb{P}(\Xi_{H, \lambda_\ell}^* \not\subset Q_{r\lambda_\ell^{-1/2}}(o)) = 0$ . Similarly, it is easy to check that  $X_{H, \lambda_\ell} \cap B_{2\lambda_\ell^{-1/2}/r}(o) = \emptyset$  implies  $\{Q_{\lambda_\ell^{-1/2}/r}(o) \subset \Xi_{H, \lambda_\ell}^*\}$ . Observe that by Lemma A.3,

$$\lim_{\lambda_\ell \rightarrow 0} \mathbb{P}(\nu_1(T^{*,(1)} \cap B_{2\lambda_\ell^{-1/2}/r}(o)) \geq 32\gamma\lambda_\ell^{-1}/r^2) = 0.$$

Furthermore,

$$\lim_{r \rightarrow \infty} \sup_{\mu \leq 32\gamma/r^2} \mathbb{P}(N_\mu \geq 1) = 0,$$

which completes the proof.  $\square$

**Remark.** A small modification of the above proof shows that Lemma A.4 remains true if  $X_{H, \lambda_\ell}$  is a homogeneous Poisson point process with intensity  $\gamma\lambda_\ell > 0$ .

We write  $d_{\text{Haus}}(\cdot, \cdot)$  for the Hausdorff distance between non-empty compact subsets of  $\mathbb{R}^2$ . Loosely speaking, the following coupling construction formalises a certain asymptotic independence of  $T^*$  and the Cox-Voronoi cell  $\Xi_{H, \lambda_\ell}^*$ . Additionally, we write  $A \oplus A' = \{a + a' : a \in A, a' \in A'\}$  for the Minkowski sum of  $A, A' \subset \mathbb{R}^2$ .

**Lemma A.5.** *For  $\lambda_\ell \in (0, 1]$  there exists a common probability space  $(\Omega, \mathcal{F}, \mathbb{P})$  on which  $T^*$ ,  $X_{H, \lambda_\ell}$ , and a homogeneous Poisson point process  $X$  with intensity  $\gamma$  are given such that the following two properties hold. If  $\Xi^*$  denotes the zero-cell of the Voronoi tessellation on  $X \cup \{o\}$ , then for every  $\varepsilon > 0$ ,*

$$\lim_{\lambda_\ell \rightarrow 0} \mathbb{P}(d_{\text{Haus}}(\sqrt{\lambda_\ell} \Xi_{H, \lambda_\ell}^*, \Xi^*) \geq \varepsilon) = 0. \quad (\text{A.7})$$

Furthermore, the probability space  $(\Omega, \mathcal{F}, \mathbb{P})$  can be chosen so that  $X$  is independent of  $T^*$ .

*Proof.* Subdivide  $Q_{\lambda_\ell^{-1}}(o)$  into  $m = \lceil \lambda_\ell^{-15/16} \rceil^2$  squares  $Q_{\lambda_\ell, 1}, \dots, Q_{\lambda_\ell, m}$  of side length  $b = \lambda_\ell^{-1} / \sqrt{m}$  and for every  $\varepsilon > 0$  define the event

$$E_\varepsilon^{(2)} = \bigcup_{i=1}^m \left\{ \left| \nu_1(T^{*,(1)} \cap Q_{\lambda_\ell, i}) - \gamma b^2 \right| \geq \varepsilon \gamma b^2 \right\}.$$

Then, Lemmas A.2 and A.3 imply the existence of a family  $\{\varepsilon_t\}_{t \in (0, 1]}$  such that

- (i)  $\varepsilon_t \in (0, 1]$  for all  $t \in (0, 1]$ ,
- (ii)  $\varepsilon_t \rightarrow 0$  as  $t \rightarrow 0$ ,
- (iii)  $\mathbb{P}(E_{\varepsilon_t}^{(2)}) \leq \varepsilon_t$  for all  $\lambda_\ell \leq t$ .

We now extend the probability space, where for simplicity, we also write  $(\Omega, \mathcal{F}, \mathbb{P})$  for the extended probability space. First, let  $X_{\lambda_\ell}^{(1)}$  be a Cox process on  $T^*$  with linear intensity  $\lambda_\ell \in (0, 1]$ . Also let  $X_{\lambda_\ell}^{(2)}$  denote a homogeneous Poisson point process with intensity  $\gamma\lambda_\ell(1 + \varepsilon_{\lambda_\ell})$  and such that additionally  $X_{\lambda_\ell}^{(2)}$  is independent of  $T^*$  and  $X_{\lambda_\ell}^{(1)}$ . Define the point process  $X_{\lambda_\ell}^{(3)}$  is obtained from  $X_{\lambda_\ell}^{(2)}$  by independent thinning with survival probability  $1/(1 + \varepsilon_{\lambda_\ell})$ . In particular,  $X = \sqrt{\lambda_\ell} X_{\lambda_\ell}^{(3)}$  constitutes a homogeneous Poisson point process with intensity  $\gamma$  and which is independent of  $T^*$ , see [7]. If  $E_{\varepsilon_{\lambda_\ell}}^{(2)}$  occurs, we simply define  $X_{H, \lambda_\ell}$  to be  $X_{\lambda_\ell}^{(1)}$ . Otherwise, we construct  $X_{\lambda_\ell}$  on each of the squares  $Q_{\lambda_\ell, 1}, \dots, Q_{\lambda_\ell, m}$  as follows. The configuration of the point

process  $X_{H,\lambda_\ell}$  inside the square  $Q_{\lambda_\ell,i}$  is obtained from  $X_{\lambda_\ell}^{(2)} \cap Q_{\lambda_\ell,i}$  by first thinning independently with survival probability  $\nu_1(T^{*(1)} \cap Q_{\lambda_\ell,i}) / ((1 + \varepsilon_{\lambda_\ell})\gamma b^2)$  and then distributing the remaining points uniformly on  $T^{*(1)} \cap Q_{\lambda_\ell,i}$ . The point process  $X_{H,\lambda_\ell}$  is obtained as the union of these thinnings and the restriction of  $X_{\lambda_\ell}^{(1)}$  to  $\mathbb{R}^2 \setminus Q_{\lambda_\ell}(o)$ . It follows from the construction that the point process  $X_{H,\lambda_\ell}$  constitutes a Cox process on  $T^{*(1)}$  with linear intensity  $\lambda_\ell$ . Next, we verify (A.7). For  $r > 0$  and  $n \geq 1$  write  $E_{n,r,\lambda_\ell}^{(3)}$  for the event  $\#(X_{\lambda_\ell}^{(2)} \cap Q_{r\lambda_\ell^{-1/2}}(o)) \geq n$ . Then, for every  $r > 0$ ,

$$\lim_{n \rightarrow \infty} \limsup_{\lambda_\ell \rightarrow 0} \mathbb{P}(E_{n,r,\lambda_\ell}^{(3)}) = 0.$$

For every  $r > 0$  denote by  $E_{r,\lambda_\ell}^{(4)}$  the event that  $E_{\varepsilon_{\lambda_\ell}}^{(2)}$  occurs or that  $E_{\varepsilon_{\lambda_\ell}}^{(2)}$  does not occur, but there exists a point of  $X_{\lambda_\ell}^{(2)} \cap Q_{r\lambda_\ell^{-1/2}}(o)$  which does not survive at least one of the two thinning operations used to create  $X_{H,\lambda_\ell}$  and  $X_{\lambda_\ell}^{(3)}$ , respectively. Then, for every  $r > 0$ ,  $n \geq 1$ ,

$$\mathbb{P}(E_{r,\lambda_\ell}^{(4)}) \leq 1 - \left( \frac{1}{1 + \varepsilon_{\lambda_\ell}} \cdot \frac{1 - \varepsilon_{\lambda_\ell}}{1 + \varepsilon_{\lambda_\ell}} \right)^n + \mathbb{P}(E_{\varepsilon_{\lambda_\ell}}^{(2)}) + \mathbb{P}(E_{n,r,\lambda_\ell}^{(3)}),$$

provided that  $\lambda_\ell > 0$  is sufficiently small. In particular,  $\lim_{\lambda_\ell \rightarrow 0} \mathbb{P}(E_{r,\lambda_\ell}^{(4)}) = 0$  for any  $r > 0$ . For  $r > 0$ , define the event  $E_{r,\lambda_\ell}^{(5)}$  by  $B_{r\lambda_\ell^{-1/2}}(o) \cap X_{\lambda_\ell}^{(2)} \neq \emptyset$ . Then,  $\lim_{r \rightarrow 0} \limsup_{\lambda_\ell \rightarrow 0} \mathbb{P}(E_{r,\lambda_\ell}^{(5)}) = 0$ .

For  $r > 0$  write  $E_{r,\lambda_\ell}^{(6)}$  for the event that  $E_{r/2,\lambda_\ell}^{(1)}$  occurs for at least one of the point processes  $X_{H,\lambda_\ell}$  or  $X_{\lambda_\ell}^{(1)}$ . From Lemma A.4, we conclude  $\lim_{r \rightarrow \infty} \limsup_{\lambda_\ell \rightarrow 0} \mathbb{P}(E_{r,\lambda_\ell}^{(6)}) = 0$ . Finally, for  $\delta, \lambda_\ell, r > 0$  let  $E_{r,\delta,\lambda_\ell}^{(7)}$  denote the event that there exists  $X_{\lambda_\ell,1}^{(3)}, X_{\lambda_\ell,2}^{(3)} \in X_{\lambda_\ell}^{(3)} \cap Q_{r\lambda_\ell}(o)$  such that

$$\#(X_{\lambda_\ell}^{(3)} \cap Q_{r\lambda_\ell^{-1/2}}(o) \cap B_{|P|+\delta\lambda_\ell^{-1/2}}(P) \setminus B_{|P|-\delta\lambda_\ell^{-1/2}}(P)) \geq 3,$$

where  $P$  denotes the intersection of the perpendicular bisectors of  $[o, X_{\lambda_\ell,1}^{(3)}]$  and  $[o, X_{\lambda_\ell,2}^{(3)}]$ . Then,  $\lim_{\delta \rightarrow 0} \limsup_{\lambda_\ell \rightarrow 0} \mathbb{P}(E_{r,\delta,\lambda_\ell}^{(7)}) = 0$ . Using these auxiliary results, we can now prove for every  $\varepsilon > 0$  that

$$\lim_{\lambda_\ell \rightarrow 0} \mathbb{P}(\Xi^* \subset \sqrt{\lambda_\ell} \Xi_{H,\lambda_\ell}^* \oplus B_\varepsilon(o)) = 1.$$

We note that similar arguments may be applied for the probability of the event  $\sqrt{\lambda_\ell} \Xi_{H,\lambda_\ell}^* \subset \Xi^* \oplus B_\varepsilon(o)$ . By the previous observations, it suffices to prove for all sufficiently large  $r_1 > 0$  and  $n \geq 1$  and all sufficiently small  $r_2, \delta > 0$  that for all sufficiently small  $\lambda_\ell > 0$  the following implication holds. If none of the events  $E_{\varepsilon_{\lambda_\ell}}^{(2)}, E_{n,r_1,\lambda_\ell}^{(3)}, E_{r_1,\lambda_\ell}^{(4)}, E_{r_2,\lambda_\ell}^{(5)}, E_{r_1,\lambda_\ell}^{(6)}, E_{r_1,\delta,\lambda_\ell}^{(7)}$  occurs, then all vertices of  $\lambda_\ell^{-1/2} \Xi^*$  are contained in  $\Xi_{H,\lambda_\ell}^* \oplus B_{\varepsilon_{\lambda_\ell}}(o)$ . To prove this implication, suppose (without loss of generality) that the Voronoi cells associated with  $X_1^{(3)}, X_2^{(3)} \in X_{\lambda_\ell}^{(3)}$  in the Voronoi tessellation on  $\{o\} \cup X_{\lambda_\ell}^{(3)}$  share a common vertex  $P$  with  $\lambda_\ell^{-1/2} \Xi^*$ . Put  $\rho = \lambda_\ell^{-1/8}$ ,  $P' = (1 - \rho/|P|)P$  and note that the proof is completed once we show  $P' \in \Xi_{H,\lambda_\ell}^*$ . Due to the occurrence of the complements of  $E_{\varepsilon_{\lambda_\ell}}^{(2)}, E_{n,r_1,\lambda_\ell}^{(3)}, E_{r_1,\lambda_\ell}^{(4)}$  and  $E_{r_1,\lambda_\ell}^{(6)}$ , there exist  $X_{1,H}, X_{2,H} \in X_{H,\lambda_\ell} = \{X_{k,H}\}_{k \geq 1}$  with  $X_{1,H}, X_1^{(3)} \in Q_{\lambda_\ell, m_1}$  and  $X_{2,H}, X_2^{(3)} \in Q_{\lambda_\ell, m_2}$  for some  $m_1, m_2 \in \{1, \dots, m\}$ . To prove  $\inf_{k \geq 1} |P' - X_{k,H}| \geq |P'|$ , we proceed in two steps. For every  $X_{k,H} \in X_{H,\lambda_\ell} \cap Q_{r_1\lambda_\ell^{-1/2}}(o)$  with  $k \notin \{1, 2\}$ ,

$$|P' - X_{k,H}| - |P'| \geq |P - X_k^{(3)}| - |P| - |X_{k,H} - X_k^{(3)}| \geq \delta\lambda_\ell^{-1/2} - |X_{k,H} - X_k^{(3)}|,$$

where the latter inequality follows from  $\{X_1^{(3)}, X_2^{(3)}\} \subset B_{|P|}(P)$  and the non-occurrence of  $E_{r_1,\delta,\lambda_\ell}^{(7)}$ . Since  $|X_{k,H} - X_k^{(3)}| \leq \sqrt{2}\lambda_\ell^{-1/16}$ , it remains to compute  $|P' - X_{1,H}| - |P'|$  and  $|P' -$

$X_{2,H} - |P'|$ . Without loss of generality, we only consider the former case. As above,

$$|P' - X_{1,H} - |P'| \geq |P' - X_1^{(3)}| - |P'| - |X_{1,H} - X_1^{(3)}|. \quad (\text{A.8})$$

Next, put  $f_a = |X_1^{(3)}|/2$  and denote by  $f_b$  the distance of  $P$  to the line segment  $[o, X_1^{(3)}]$ . Then, Figure A.2 yields  $|P' - X_1^{(3)}|^2 = (f_a + \rho f_a/|P|)^2 + (f_b - \rho f_b/|P|)^2$ . In particular,

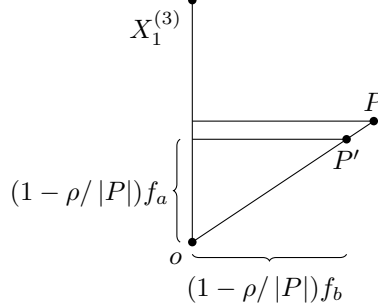


FIGURE A.2. Configuration in the proof of Lemma A.5

$$\begin{aligned} |P' - X_1^{(3)}|^2 - |P'|^2 &= (f_a + \rho f_a/|P|)^2 + (f_b - \rho f_b/|P|)^2 - (|P| - \rho)^2 \\ &= 2\rho(f_a^2/|P| - f_b^2/|P| + (f_a^2 + f_b^2)/|P|), \end{aligned}$$

which is equal to  $4\rho f_a^2/|P|$ . Therefore,

$$|P' - X_1^{(3)}| - |P'| = \frac{4\rho f_a^2/|P|}{|P' - X_1^{(3)}| + |P'|} \geq \rho \frac{r_2^2/(2r_1)}{4r_1} = \rho r_2^2/(8r_1^2).$$

Inserting this into (A.8) and recalling that  $\rho = \lambda_\ell^{-1/8}$ , while  $|X_{1,H} - X_1^{(1)}| \leq \sqrt{2}\lambda_\ell^{-1/16}$  concludes the proof of Lemma A.5.  $\square$

## APPENDIX B. PROOF OF LEMMAS 4.2 AND 4.3

Recall that we assumed the points  $(L''_{1,\lambda_\ell}, L''_{2,\lambda_\ell})$  to be distributed uniformly in  $\Xi_{H,\lambda_\ell}^*$ , while the points  $(\lambda_\ell^{-1/2}L'_1, \lambda_\ell^{-1/2}L'_2)$  are distributed uniformly in  $\lambda_\ell^{-1/2}\Xi^*$ . Furthermore, recall that in Lemma A.5 we established a coupling between  $\Xi_{H,\lambda_\ell}^*$  and  $\lambda_\ell^{-1/2}\Xi^*$  such that with a probability tending to 1 the cells  $\Xi_{H,\lambda_\ell}^*$  and  $\lambda_\ell^{-1/2}\Xi^*$  are close in the Hausdorff metric. In the following result, we extend this coupling to the derived point pairs  $(L''_{1,\lambda_\ell}, L''_{2,\lambda_\ell})$  and  $(\lambda_\ell^{-1/2}L'_1, \lambda_\ell^{-1/2}L'_2)$ . In the following  $\nu_2(\cdot)$  denotes the Lebesgue measure in  $\mathbb{R}^2$ .

*Proof of Lemma 4.2.* The proof is based on the observation that the measures  $\nu_1(T^{*(1)} \cap \cdot)$  and  $\gamma\nu_2(\cdot)$  exhibit a similar asymptotic behavior. To be more precise, for  $z \in \mathbb{Z}^2$  put

$$p_z = \nu_1(T^{*(1)} \cap Q_{\lambda_\ell^{-1/4}}(\lambda_\ell^{-1/4}z) \cap \Xi_{H,\lambda_\ell}^*) / \nu_1(T^{*(1)} \cap \Xi_{H,\lambda_\ell}^*)$$

and

$$p''_z = \nu_2(Q_{\lambda_\ell^{-1/4}}(\lambda_\ell^{-1/4}z) \cap \Xi_{H,\lambda_\ell}^*) / \nu_2(\Xi_{H,\lambda_\ell}^*).$$

Conditional on  $T^*$  and  $X_{H,\lambda_\ell}$  we may create a sample of  $L_{1,\lambda_\ell}$  by selecting an element  $(Z, R)$  uniformly from the set  $\{(z, r) \in \mathbb{Z}^2 \times [0, 1] : r \leq p_z\}$  and choosing  $L_{1,\lambda_\ell}$  uniformly from  $T^* \cap Q_{\lambda_\ell^{-1/4}}(\lambda_\ell^{-1/4}Z) \cap \Xi_{H,\lambda_\ell}^*$ . Similarly, to create a sample of  $L''_{1,\lambda_\ell}$  conditional on  $T^*$  and  $X_{H,\lambda_\ell}$ , we first select a point  $(Z'', R'')$  uniformly from the set  $\{(z, r) \in \mathbb{Z}^2 \times [0, 1] : r \leq p''_z\}$  and then choose  $L''_{1,\lambda_\ell}$  uniformly from  $Q_{\lambda_\ell^{-1/4}}(\lambda_\ell^{-1/4}Z'') \cap \Xi_{H,\lambda_\ell}^*$ . Using this framework,  $L_{1,\lambda_\ell}$  and  $L''_{1,\lambda_\ell}$  can be coupled via rejection sampling. Indeed, to create a sample of  $(Z, R)$  we may repeatedly

draw uniformly from  $\{(z, r) \in \mathbb{Z}^2 \times [0, 1] : r \leq \max\{p_z, p'_z\}\}$  until we obtain an element of  $\{(z, r) \in \mathbb{Z}^2 \times [0, 1] : r \leq p_z\}$ . A similar remark applies to  $(Z'', R'')$ . For the remaining points  $L_{2, \lambda_\ell}, L''_{2, \lambda_\ell}$ , we proceed similarly. Additionally, we obtain

$$\begin{aligned} \mathbb{P}(|L_{1, \lambda_\ell} - L''_{1, \lambda_\ell}| \geq \sqrt{2}\lambda_\ell^{-1/4} \mid T^*, X_{H, \lambda_\ell}) &\leq \mathbb{P}(Z \neq Z'' \mid T^*, X_{H, \lambda_\ell}) \\ &\leq 2 \sum_{z \in A_1} |p_z - p''_z| + 2 \sum_{z \in A_2} |p_z - p''_z|, \end{aligned} \quad (\text{B.1})$$

where we put

$$A_1 = \{z \in \mathbb{Z}^2 : Q_{\lambda_\ell^{-1/4}}(\lambda_\ell^{-1/4}z) \subset \Xi_{H, \lambda_\ell}^*\}$$

and

$$A_2 = \{z \in \mathbb{Z}^2 : Q_{\lambda_\ell^{-1/4}}(\lambda_\ell^{-1/4}z) \cap \partial\Xi_{H, \lambda_\ell}^* \neq \emptyset\},$$

where  $\partial\Xi_{H, \lambda_\ell}^*$  denotes the topological boundary of  $\Xi_{H, \lambda_\ell}^*$ . Hence, our strategy is to define a suitable family of events  $\{E_{\lambda_\ell}^{(1)}\}_{\lambda_\ell \in (0, 1]}$  such that

- (i)  $E_{\lambda_\ell}^{(1)}$  is measurable with respect to the  $\sigma$ -algebra generated by  $T^*$  and  $X_{H, \lambda_\ell}$ ,
- (ii)  $\mathbb{P}(E_{\lambda_\ell}^{(1)}) \rightarrow 1$  as  $\lambda_\ell \rightarrow 0$ ,
- (iii) under  $E_{\lambda_\ell}^{(1)}$  the two summands in (B.1) tend to 0 as  $\lambda_\ell \rightarrow 0$ .

As the value of  $\lambda_\ell$  will be clear from the context, we write  $Q_z$  for  $Q_{\lambda_\ell^{-1/4}}(\lambda_\ell^{-1/4}z)$  in the following.

Before we provide a precise definition of the events  $\{E_{\lambda_\ell}^{(1)}\}_{\lambda_\ell \in (0, 1]}$ , it is convenient to make two preliminary observations. First, we claim that there exists a constant  $c_1 > 0$  such that for all  $\lambda_\ell \in (0, 1)$  and  $r \geq 1$ , if  $\Xi_{H, \lambda_\ell}^* \subset Q_{r\lambda_\ell^{-1/2}}(o)$ , then  $n_2 \leq c_1 r \lambda_\ell^{-1/4}$ , where  $n_2 = \#A_2$ . Indeed, from convexity of  $\Xi_{H, \lambda_\ell}^*$  we conclude that for every  $z \in A_2$  there exists  $z' \in \mathbb{Z}^2$  such that  $|z - z'|_\infty = 1$  and  $Q_{z'} \subset (\Xi_{H, \lambda_\ell}^* \oplus B_{3\lambda_\ell^{-1/4}}(o)) \setminus \Xi_{H, \lambda_\ell}^*$ . Hence, again using convexity of  $\Xi_{H, \lambda_\ell}^*$ ,

$$n_2 \leq 9 \frac{\nu_2(\Xi_{H, \lambda_\ell}^* \oplus B_{3\lambda_\ell^{-1/4}}(o)) - \nu_2(\Xi_{H, \lambda_\ell}^*)}{\lambda_\ell^{-1/2}} \leq 9\pi \frac{(r\lambda_\ell^{-1/2} + 3\lambda_\ell^{-1/4})^2 - (r\lambda_\ell^{-1/2})^2}{\lambda_\ell^{-1/2}},$$

which is at most  $144\pi r \lambda_\ell^{-1/4}$ . In the second auxiliary result, we claim that there exists a constant  $c_2 > 0$  such that for all  $r \geq 1$  and  $16\lambda_\ell \leq r^{-4}$  the following implication is true. If

- (i)  $Q_{1/r}(o) \subset \sqrt{\lambda_\ell} \Xi_{H, \lambda_\ell}^*$ , and
- (ii)  $\nu_1(T^{*,(1)} \cap Q_z) \in (\frac{\gamma}{2}\lambda_\ell^{-1/2}, 2\gamma\lambda_\ell^{-1/2})$  for all  $z \in \mathbb{Z}^2$  with  $Q_z \subset Q_{\lambda_\ell^{-1/2}/r}(o)$ ,

then  $\min\{\nu_2(\Xi_{H, \lambda_\ell}^*), \nu_1(T^{*,(1)} \cap \Xi_{H, \lambda_\ell}^*)\} \geq c_2 r^{-2} \lambda_\ell^{-1}$ . First, note that (i) immediately implies the lower bound  $\nu_2(\Xi_{H, \lambda_\ell}^*) \geq r^{-2} \lambda_\ell^{-1}$ . For the second bound, observe that as  $r^{-1} \lambda_\ell^{-1/2} \geq 2\lambda_\ell^{-1/4}$ , the square  $Q_{r^{-1}\lambda_\ell^{-1/2}}(o)$  contains at least  $(r^{-1}/2)^2 \lambda_\ell^{-1/2}$  smaller squares of the form  $Q_z$ ,  $z \in \mathbb{Z}^2$ , so that  $\nu_1(T^{*,(1)} \cap \Xi_{H, \lambda_\ell}^*) \geq (r^{-1}/2)^2 \gamma \lambda_\ell^{-1/2}$ . Next, we provide a precise definition of the family of events  $\{E_{\lambda_\ell}^{(1)}\}_{\lambda_\ell \in (0, 1]}$  and then show that it has the desired properties. First, Lemmas A.3 and A.4 imply the existence of families  $\{\varepsilon_t\}_{t \in (0, 1]}$  and  $\{r_t\}_{t \in (0, 1]}$  such that

- (i)  $\varepsilon_t \in (0, 1]$  and  $r_t \in [1, \infty)$  for all  $t \in (0, 1]$ ,
- (ii)  $\varepsilon_1 = 1$  and  $r_1 = 1$ ,
- (iii) the family  $\{\varepsilon_t\}_{t \in (0, 1]}$  is increasing in  $t$  and  $\lim_{t \rightarrow 0} \varepsilon_t = 0$ ,
- (iv) the family  $\{r_t\}_{t \in (0, 1]}$  is decreasing in  $t$  and  $\lim_{t \rightarrow 0} r_t = \infty$ ,
- (v)  $\mathbb{P}(Q_{1/r_t}(o) \subset \sqrt{\lambda_\ell} \Xi_{H, \lambda_\ell}^* \subset Q_{r_t}(o)) \geq 1 - \varepsilon_t$  for all  $t \in (0, 1]$  and  $\lambda_\ell \leq t$ ,
- (vi)  $\mathbb{P}\left(\bigcap_{z \in A(\lambda_\ell, r_t)} \left\{ \left| \nu_1(T^{*,(1)} \cap Q_z) - \gamma \lambda_\ell^{-1/2} \right| \leq \frac{\gamma}{2} r_t^{-5} \lambda_\ell^{-1/2} \right\}\right) \geq 1 - \varepsilon_t$  for all  $t \in (0, 1]$  and  $\lambda_\ell \leq t$ , where  $A(\lambda_\ell, r_t) = \{z \in \mathbb{Z}^2 : Q_z \cap Q_{r_t \lambda_\ell^{-1/2}}(o) \neq \emptyset\}$ .

Furthermore, for  $\lambda_\ell \in (0, 1/64]$ , we put  $t^*(\lambda_\ell) = \inf\{t \geq \lambda_\ell : r_t^{-16} \geq \lambda_\ell\}$  and  $r^*(\lambda_\ell) = r_{t^*(\lambda_\ell)}$ . Using this notation, we define

$$E_{\lambda_\ell}^{(1)} = \left\{ Q_{1/r^*(\lambda_\ell)}(o) \subset \sqrt{\lambda_\ell} \Xi_{H, \lambda_\ell}^* \subset Q_{r^*(\lambda_\ell)}(o) \right\} \\ \cap \bigcap_{z \in A(\lambda_\ell, r^*(\lambda_\ell))} \left\{ |\nu_1(T^{*,(1)} \cap Q_z) - \gamma \lambda_\ell^{-1/2}| \leq \frac{\gamma}{2} r^*(\lambda_\ell)^{-5} \lambda_\ell^{-1/2} \right\}.$$

Then, clearly,  $E_{\lambda_\ell}^{(1)}$  is measurable with respect to the  $\sigma$ -algebra generated by  $T^*$  and  $X_{H, \lambda_\ell}$ . Additionally, the above discussion shows  $\mathbb{P}(E_{\lambda_\ell}^{(1)}) \rightarrow 1$  as  $\lambda_\ell \rightarrow 0$  and it remains to verify that under  $E_{\lambda_\ell}^{(1)}$  the two sums in (B.1) tend to 0 as  $\lambda_\ell \rightarrow 0$ . We begin by considering the second sum. Under  $E_{\lambda_\ell}^{(1)}$ ,

$$\sum_{z \in A_2} |p_z - p_z''| \leq c_1 r^*(\lambda_\ell) \lambda_\ell^{-1/4} \max_{z \in A_2} (p_z + p_z'') \leq c_1 r^*(\lambda_\ell) \lambda_\ell^{-1/4} \cdot c_2^{-1} r^*(\lambda_\ell)^2 \lambda_\ell \cdot (1 + 2\gamma) \lambda_\ell^{-1/2}$$

which is at most  $c_1 c_2^{-1} (1 + 2\gamma) r^*(\lambda_\ell)^3 \lambda_\ell^{1/4}$ , and this expression tends to 0 as  $\lambda_\ell \rightarrow 0$ , by the definition of  $r^*(\lambda_\ell)$ . Finally, we consider the first sum in (B.1). Note that under  $E_{\lambda_\ell}^{(1)}$ ,

$$\sum_{z \in A_1} |p_z - p_z''| \leq \nu_1(T^{*,(1)} \cap \Xi_{H, \lambda_\ell}^*)^{-1} \sum_{z \in A_1} |\nu_1(T^{*,(1)} \cap Q_z) - \gamma \lambda_\ell^{-1/2}| \\ + n_1 \lambda_\ell^{-1/2} \nu_1(T^{*,(1)} \cap \Xi_{H, \lambda_\ell}^*)^{-1} \nu_2(\Xi_{H, \lambda_\ell}^*)^{-1} |\gamma \nu_2(\Xi_{H, \lambda_\ell}^*) - \nu_1(T^{*,(1)} \cap \Xi_{H, \lambda_\ell}^*)|,$$

where  $n_1 = \#A_1$ . We consider bounds for the latter two summands separately. First, observe that the inclusion  $\bigcup_{z \in A_1} Q_z \subset \Xi_{H, \lambda_\ell}^*$  implies  $n_1 \leq \nu_2(\Xi_{H, \lambda_\ell}^*) \sqrt{\lambda_\ell}$ . Next, if

- (i)  $Q_{1/r^*(\lambda_\ell)}(o) \subset \sqrt{\lambda_\ell} \Xi_{H, \lambda_\ell}^* \subset Q_{r^*(\lambda_\ell)}(o)$  and
- (ii)  $|\nu_1(T^{*,(1)} \cap Q_z) - \gamma \lambda_\ell^{-1/2}| \leq \frac{\gamma}{2} r^*(\lambda_\ell)^{-5} \lambda_\ell^{-1/2}$  for all  $z \in \mathbb{Z}^2$  with  $Q_z \subset Q_{r^*(\lambda_\ell) \lambda_\ell^{-1/2}}(o)$ ,

then

$$\nu_1(T^{*,(1)} \cap \Xi_{H, \lambda_\ell}^*)^{-1} \sum_{z \in A_1} |\nu_1(T^{*,(1)} \cap Q_z) - \gamma \lambda_\ell^{-1/2}| \\ \leq c_2^{-1} r^*(\lambda_\ell)^2 \lambda_\ell \cdot \nu_2(\Xi_{H, \lambda_\ell}^*) \sqrt{\lambda_\ell} \cdot \frac{\gamma}{2} r^*(\lambda_\ell)^{-5} \lambda_\ell^{-1/2},$$

which is at most  $\frac{\gamma}{2} c_2^{-1} r^*(\lambda_\ell)^{-1}$ , and this expression tends to 0 as  $\lambda_\ell \rightarrow 0$ . We also conclude from  $n_1 \leq \nu_2(\Xi_{H, \lambda_\ell}^*) \sqrt{\lambda_\ell}$  that the second summand is bounded from above by

$$(\lambda_\ell \nu_1(T^{*,(1)} \cap \Xi_{H, \lambda_\ell}^*))^{-1} \lambda_\ell |\gamma \nu_2(\Xi_{H, \lambda_\ell}^*) - \nu_1(T^{*,(1)} \cap \Xi_{H, \lambda_\ell}^*)| \\ \leq c_2^{-1} r^*(\lambda_\ell)^2 \lambda_\ell \left| \gamma \nu_2(\Xi_{H, \lambda_\ell}^*) - \nu_1(T^{*,(1)} \cap \Xi_{H, \lambda_\ell}^*) \right|.$$

Finally, note that

$$r^*(\lambda_\ell)^2 \lambda_\ell |\gamma \nu_2(\Xi_{H, \lambda_\ell}^*) - \nu_1(T^{*,(1)} \cap \Xi_{H, \lambda_\ell}^*)| \leq r^*(\lambda_\ell)^2 \lambda_\ell \sum_{z \in A_1} |\gamma \lambda_\ell^{-1/2} - \nu_1(T^{*,(1)} \cap Q_z)| \\ + r^*(\lambda_\ell)^2 \lambda_\ell \sum_{z \in A_2} (\gamma \lambda_\ell^{-1/2} + \nu_1(T^{*,(1)} \cap Q_z)),$$

which is at most  $\frac{\gamma}{2} n_1 \sqrt{\lambda_\ell} r^*(\lambda_\ell)^{-3} + 3n_2 \gamma \sqrt{\lambda_\ell} r^*(\lambda_\ell)^2$ , and tends to 0 as  $\lambda_\ell \rightarrow 0$ . This completes the proof of Lemma 4.2.  $\square$

*Proof of Lemma 4.3.* In the following, we always consider  $\Xi_{H, \lambda_\ell}^*$  and  $\Xi^*$  as random sets defined on the common probability space  $(\Omega, \mathcal{F}, \mathbb{P})$  resulting from the coupling provided by Lemma A.5. Using rejection sampling, conditional on  $T^*$  and  $X_{H, \lambda_\ell}$ , we may create a sample of  $L''_{1, \lambda_\ell}$  by repeatedly drawing uniformly distributed random vectors on  $\Xi_{H, \lambda_\ell}^* \cup \lambda_\ell^{-1/2} \Xi^*$  until we obtain a

random vector located in  $\Xi_{H,\lambda_\ell}^*$ . For the random vector  $\lambda_\ell^{-1/2}L'_1$  we can proceed similarly. The same approach can be used for the remaining random vectors  $L'_2, L''_{2,\lambda_\ell}$ . Hence,

$$\begin{aligned} \mathbb{P}(L''_{1,\lambda_\ell} \neq \lambda_\ell^{-1/2}L'_1 \mid T^*, X_H) &\leq 2 \left( 1 - \frac{\nu_2(\Xi_{H,\lambda_\ell}^* \cap \lambda_\ell^{-1/2}\Xi^*)}{\nu_2(\Xi_{H,\lambda_\ell}^* \cup \lambda_\ell^{-1/2}\Xi^*)} \right) \\ &= 2 \frac{\nu_2(\Xi_{H,\lambda_\ell}^* \setminus \lambda_\ell^{-1/2}\Xi^*) + \nu_2(\lambda_\ell^{-1/2}\Xi^* \setminus \Xi_{H,\lambda_\ell}^*)}{\nu_2(\Xi_{H,\lambda_\ell}^* \cup \lambda_\ell^{-1/2}\Xi^*)} \\ &\leq 2 \frac{\nu_2(\sqrt{\lambda_\ell}\Xi_{H,\lambda_\ell}^* \setminus \Xi^*)}{\nu_2(\Xi^*)} + 2 \frac{\nu_2(\Xi^* \setminus \sqrt{\lambda_\ell}\Xi_{H,\lambda_\ell}^*)}{\nu_2(\Xi^*)}. \end{aligned} \quad (\text{B.2})$$

Next, Lemmas A.4 and A.5 imply the existence of families  $\{\varepsilon_t\}_{t \in (0,1]}$  and  $\{r_t\}_{t \in (0,1]}$  such that

- (i)  $\varepsilon_t \in (0, 1]$  and  $r_t \in [1, \infty)$  for all  $t \in (0, 1]$ ,
- (ii)  $\varepsilon_1 = 1$  and  $r_1 = 1$ ,
- (iii) the family  $(\varepsilon_t)_{t \in (0,1]}$  is increasing in  $t$  and  $\lim_{t \rightarrow 0} \varepsilon_t = 0$ ,
- (iv) the family  $(r_t)_{t \in (0,1]}$  is decreasing in  $t$  and  $\lim_{t \rightarrow 0} r_t = \infty$ ,
- (v)  $\mathbb{P}(Q_{1/r_t}(o) \subset \Xi^* \subset Q_{r_t}(o)) \geq 1 - \varepsilon_t$  for all  $t \in (0, 1]$  and  $\lambda_\ell \leq t$ ,
- (vi)  $\mathbb{P}(d_{\text{Haus}}(\sqrt{\lambda_\ell}\Xi_{H,\lambda_\ell}^*, \Xi^*) \leq r_t^{-4}) \geq 1 - \varepsilon_t$  for all  $t \in (0, 1]$  and all  $\lambda_\ell \leq t$ .

For  $\lambda_\ell \in (0, 1]$ , we put  $t^*(\lambda_\ell) = \inf\{t \geq \lambda_\ell : r_t^{-16} \geq \lambda_\ell\}$  and  $r^*(\lambda_\ell) = r_{t^*(\lambda_\ell)}$ . Using this notation, we define the event  $E_{\lambda_\ell}^{(2)}$  by

$$\{Q_{1/r^*(\lambda_\ell)}(o) \subset \sqrt{\lambda_\ell}\Xi_{H,\lambda_\ell}^* \subset Q_{r^*(\lambda_\ell)}(o)\} \cap \{d_{\text{Haus}}(\sqrt{\lambda_\ell}\Xi_{H,\lambda_\ell}^*, \Xi^*) \leq r^*(\lambda_\ell)^{-4}\},$$

so that  $\mathbb{P}(E_{\lambda_\ell}^{(2)}) \rightarrow 1$  as  $\lambda_\ell \rightarrow 0$ . Moreover, if  $E_{\lambda_\ell}^{(2)}$  occurs, then

$$\begin{aligned} \frac{\nu_2(\sqrt{\lambda_\ell}\Xi_{H,\lambda_\ell}^* \setminus \Xi^*)}{\nu_2(\Xi^*)} &\leq \frac{\nu_2(\Xi^* \oplus B_{r^*(\lambda_\ell)^{-4}}(o)) - \nu_2(\Xi^*)}{\nu_2(\Xi^*)} \\ &\leq \frac{4\pi r^*(\lambda_\ell)^{-3}}{r^*(\lambda_\ell)^{-2}}, \end{aligned}$$

and the latter expression tends to 0 as  $\lambda_\ell \rightarrow 0$ . Observing that a similar argument applies to the second expression in (B.2) completes the proof.  $\square$

## REFERENCES

- [1] Aldous D., Shun J. Connected spatial networks over random points and a route-length statistic. *Statistical Science* 25:275–288, 2010.
- [2] Baccelli F., Błaszczyszyn B. *Stochastic Geometry and Wireless Networks: Vol. I/II*. Now Publishers, Norwell, 2009.
- [3] Baumeier B., Stenzel O., Poelking C., Andrienko D., Schmidt V. Stochastic modeling of molecular charge transport networks. *Physical Review B* 86:184–202, 2012.
- [4] Baryshnikov Y., Eichelsbacher P., Schreiber T., Yukich J. E. Moderate deviations for some point measures in geometric probability. *Annales de l'Institut Henri Poincaré Probabilités et Statistiques*, 44:422–446, 2008.
- [5] Bose P., Devroye L., Evans W., Kirkpatrick D. On the spanning ratio of gabriel graphs and  $\beta$ -skeletons. In: Proceedings of the 5th Latin American Symposium on Theoretical Informatics (LATIN'02), Lecture Notes in Computer Science 2286:479–493, Springer, Berlin, 2002.
- [6] Chiu S.N., Stoyan D., Kendall W.S., Mecke J. *Stochastic Geometry and its Applications*. J. Wiley & Sons, Chichester, 2013.
- [7] Daley D.J., Vere-Jones D. *An Introduction to the Theory of Point Processes*. Vol. I/II, Springer, New York, 2005/08.
- [8] Eichelsbacher P., Schreiber T. Process level moderate deviations for stabilizing functionals. *ESAIM Probability and Statistics*, 14:1–15, 2010.
- [9] Friedman J.H., Rafsky L.C. Multivariate generalizations of the Wald-Wolfowitz and Smirnov two-sample tests. *The Annals of Statistics*, 7:967–717, 1979.
- [10] Hirsch C., Neuhäuser D., Gloaguen C., Schmidt V. First-passage percolation on random geometric graphs and an application to shortest-path trees. *Advances in Applied Probability* 47, 2015 (in print).

- [11] Hirsch C., Neuhäuser D., Gloaguen C., Schmidt V. Asymptotic properties of Euclidean shortest-path trees in random geometric graphs. Preprint (submitted).
- [12] Hofert J.M. *Sampling Nested Archimedean Copulas with Applications to CDO Pricing*. Südwestdeutscher Verlag für Hochschulschriften AG & Co. KG, Saarbrücken, 2010.
- [13] Illian J., Penttinen A., Stoyan H., Stoyan D. *Statistical Analysis and Modelling of Spatial Point Patterns*. J. Wiley & Sons, Chichester, 2008.
- [14] Linnik J. V. On the probability of large deviations for the sums of independent variables. In Neyman J., editor, *Proceedings of the 4th Berkeley Symposium on Mathematical Statistics and Probability*, pages 289–306. University of California Press, Berkeley, 1961.
- [15] Mai J.-F., Scherer M. *Simulating Copulas: Stochastic Models, Sampling Algorithms, and Applications*. Imperial College Press, London, 2012.
- [16] Nagel W., Weiß V. Crack STIT tessellations: Characterization of stationary random tessellations stable with respect to iteration. *Advances in Applied Probability*, 37:859–883, 2005.
- [17] Nahapetian B. *Limit Theorems and Some Applications in Statistical Physics*. Teubner, Stuttgart, 1991.
- [18] Nelsen R.B. *An Introduction to Copulas*. Springer, New York, 2006.
- [19] Neuhäuser D., Hirsch C., Gloaguen C., Schmidt V. On the distribution of typical shortest-path lengths in connected random geometric graphs. *Queueing Systems* 71:199-220, 2012.
- [20] Neuhäuser D., Hirsch C., Gloaguen C., Schmidt V. A parametric copula approach for modelling shortest-path trees in telecommunication networks. In: A. Dudin and K. Turck (eds.) *Analytical and Stochastic Modeling Techniques and Applications. Lecture Notes in Computer Science* 7984, Springer, Berlin 2013, 324-336.
- [21] Neuhäuser D., Hirsch C., Gloaguen C., Schmidt V. Joint distributions for total lengths of shortest-path trees in telecommunication networks. *Annals of Telecommunications* (in print).
- [22] Norros I., Kuusela P., Innamaa S., Pilli-Sihvola E., Rajamäki R. The Palm distribution of traffic conditions and its application to incident risk assessment. Preprint (submitted).
- [23] Savu C., Trede M. Hierarchies of Archimedean copulas. *Quantitative Finance*, 10:295-304, 2010.
- [24] Schneider R., Weil W. *Stochastic and Integral Geometry*. Springer, Berlin, 2008.
- [25] Thäle C., Redenbach C. On the arrangement of cells in planar STIT and Poisson line tessellations. *Methodology and Computing in Applied Probability*, 15:643-654, 2013.
- [26] Voss F., Gloaguen C., Schmidt V. Scaling limits for shortest path lengths along the edges of stationary tessellations. *Advances in Applied Probability*, 42:936-952, 2010.